Title: Review of supercritical water gasification with lignocellulosic real biomass as the feedstocks: process parameters, biomass composition, catalyst development, reactor design and its challenges

Abstract

Supercritical water gasification (SCWG) is a combined thermal decomposition and hydrolysis process for converting wet biomass feedstock with high water content potentially (80wt%) to syngas. The process bypasses the need for an energy intensive pre-drying step and also needs relatively shorter residence times (of the order of seconds to minutes) when compared to conventional gasification. The main target of SCWG is to obtain syngas rich in hydrogen whilst minimising char formation. In recent years, SCWG studies have advanced from using model compounds (e.g. glucose and cellulose) towards the use of real biomass and its waste (e.g. sugarcane trash). The use of biomass as a feedstock creates real opportunities for the technology since it is available in some form, regardless of location. This review discusses the findings from SCWG studies that have used real biomass as a feedstock. The effects of reaction temperature, pressure, residence time and feedstock concentration to the hydrogen yields are presented. The relationship between the main components in biomass (cellulose, hemicellulose and lignin) and hydrogen yields are also discussed. Homogeneous and heterogeneous catalysts have been used to enhance SCWG with real biomass feedstock and the benefits of these approaches are also considered. The economic benefits of running the catalytic SCWG at 400 °C compared to non-catalytic operation at 600 °C is evaluated. Reactor configuration and process conditions vary across the literature, and various authors describe the associated challenges (char formation and plugging, corrosion) as well as promising solutions to tackle these key challenges.

Keywords: supercritical water gasification, hydrogen, lignocellulosic biomass, hydrothermal, catalysts

Abbreviations:

AC = activated carbon

α-Al_2O_3 = aluminium oxide

CaO = calcium oxide

CAPEX = capital expenditure

CeO_2 = cerium (IV) oxide

CH_4 = methane

CMC = carboxymethyl cellulose

CNTs = carbon nanotubes

Co = cobalt

CO = carbon monoxide

CO_2 = carbon dioxide

Cu = copper

Fe = iron

H_2 = hydrogen

5-HMF = 5-(hydroxymethyl)furfural

HE = heat exchanger

HGE = hydrogen gasification efficiency

HP = high pressure

La = lanthanum

LDPE = low density polyethylene

K_2CO_3 = potassium carbonate

MgO = magnesium oxide

NCW = near critical water

Ni = nickel

OPEX = operating expenditure

PR-BM = Peng Robinson with Boston Mathias mixing rules

Ru = ruthenium

SbCWG = subcritical water gasification

SCWG = supercritical water gasification

SCWO = supercritical water oxidation

SEM = scanning electron miscroscopy

SS = stainless steel

TiO_2 = titanium dioxide

TWR = transpiring wall reactor

WGS = water-gas shift

ZnO = zinc oxide

ZrO_2 = zirconium dioxide

1. Introduction

Interest in sustainable supercritical water gasification (SCWG) for industrial-scale applications has been growing over the last decade due to the increased focus on generating low-cost "green" hydrogen from renewable and environmentally friendly feedstocks such as biomass. SCWG is a thermochemical conversion of wet biomass using supercritical water in order to degrade the biomass into gaseous (mainly syngas), liquid and solid (char) bio-products. The major advantage of SCWG is that the wet biomass can be directly gasified without an energy intensive drying step. Biomass can contain up to 80% moisture and the introduction of a drying process can potentially make any conversion process non-viable economically.

Biomass itself is quite a broad classification of materials, available across the whole world and is therefore quite heterogeneous depending on the feedstocks and location. In order to reduce the complexity, most of the SCWG studies in literature tend to focus on model compounds that tend to make up the majority of most biomass materials, namely cellulose, hemicellulose and lignin. Glucose, xylose, and phenolic compounds are the monomers of cellulose, hemicellulose, and lignin, respectively and both monomers and polymers have been used as biomass model compounds. The main thermochemical reactions involved in SCWG [1] are listed as below.

$$Steam\ reforming\ reaction\ 1\text{: } C_xH_yO_z + (2x - z)H_2O \rightarrow xCO_2 + (2x - z + y/2)H_2 \quad (1)$$

$$Steam\ reforming\ reaction\ 2\text{: } C_xH_yO_z + (x - z)H_2O \rightarrow xCO + (x - z + y/2)H_2 \quad (2)$$

$$Water\ gas\ shift\ (WGS)\ reaction\text{: } CO + H_2O \leftrightarrow H_2 + CO_2 \quad (3)$$

$$Methanation\ reaction\ of\ CO_2\text{: } CO_2 + 4H_2 \leftrightarrow CH_4 + 2H_2O \quad (4)$$

$$Methanation\ reaction\ of\ CO\text{: } CO + 3H_2 \leftrightarrow CH_4 + H_2O \quad (5)$$

Hydrogen rich syngas (H_2, CH_4, CO_2 and CO) is the target of most SCWG studies. Many SCWG studies were performed with catalysts in order to lower the reaction temperature, promote WGS reaction to obtain high hydrogen yield and reduce char and tar formation. In all cases the yields and composition of gaseous products, aqueous products and solid residue obtained via SCWG are identified by different analytical techniques. Gaseous products are normally identified by gas chromatography and generally found to consist mainly of

hydrogen (H_2), carbon dioxide (CO_2), methane (CH_4), carbon monoxide (CO) and C_2–C_4 compounds. Aqueous products are analysed via total organic carbon test and high performance liquid chromatography, and mainly found to consist of carboxylic acids (hydroxyacetic acid, formic acid and acetic acid), furfurals, phenols (phenol and cresols), aldehydes (formaldehyde and acetaldehyde) [2]. There are limited number of studies that quantify and analyse the solid products (char) generated during the SCWG process.

In the past 15 years SCWG studies have moved away from model compounds towards the use of real lignocellulosic biomass (e.g. agricultural residues, forestry biomass, industrial biomass waste, food processing waste). This has been driven by the need to understand the chemistry and reaction mechanisms that allow biomass to convert to syngas. SCWG of real biomass is considerably more challenging than model compounds due to the complex nature of real biomass feedstock and multiple reactions happening in solid and liquid phases concurrently to yield gas, liquid, and solid char [3]. Specific differences include: (i) Real biomass contains lignin which is difficult to gasify whereas model compounds without lignin tend to gasify more easily and produce a higher hydrogen content. (ii) Model compounds can be more easily dissolved in water compared to real biomass. (iii) With real biomass, the water in the mixture of biomass and water feedstock might be evaporated readily during the reaction, the dissolution of the solid material might not occur even if the biomass particles are fine and well mixed [4].

Several review papers about SCWG have been published focusing on the SCWG reaction pathway for the conversion of model compounds and certain biomass to gaseous products [3][5], degradation routes of biomass model compounds [6], types of catalysts used in SCWG [6][7][8], the reaction mechanisms for catalytic SCWG [9], the effects of process parameters on the gasification efficiency [6][8][9], the effects of biomass components and reaction conditions to the chemical reaction pathways of SCWG [8], design strategies and operational challenges for laboratory scale continuous flow reactor [5][10]. Those papers predominantly focus on model compounds as feedstocks with only a small number using real biomass, microalgae, sewage sludge and industrial wastewater as feedstocks.

This review paper focusses on the SCWG of real biomass, specifically looking at biomass composition, reactor design, type of catalyst, operating conditions, hydrogen yield and char formation. The effect of process parameters such as temperature, pressure, residence time and feedstock concentration, that significantly affect

the gasification efficiency and hydrogen yield, are presented. The effect of biomass composition (cellulose, hemicellulose and lignin content) to the gasification efficiency is also discussed as this information is useful when selecting real biomass as a feedstock for a large scale SCWG application. Types of the homogeneous catalysts (alkali-based catalysts) and heterogeneous catalysts (metal-based with support material, natural mineral, red mud and hydrochars) are also considered along the benefits and drawbacks of their use and impact on hydrogen yield. The economic benefit of catalytic SCWG at 400 °C versus non-catalytic SCWG at 600 °C is assessed via Aspen Plus. Different types of reactor have been used in the literature and their potential to solve associated problems, particularly char formation and plugging and reactor corrosion, are discussed in detail. A promising approach to tackle the energy inefficiency in SCWG is also presented. This review provides some insight into the SCWG of real biomass, the encountered technical challenges, and the potential solutions to tackle these challenges.

2. Supercritical Water Gasification Variables

2.1 The effect of temperature to the gasification efficiency

In SCWG process, temperature is one of the significant parameters that directly affects gasification efficiency and hydrogen yield. Some batch SCWG experiments have investigated the impact of temperature on the hydrogen yield by using real biomass as a feedstock.

Hydrogen yields of almond shell (6.8 wt% to 13.5 wt%), cotton cocoon shell (5.9 wt% to 11.1 wt%), hazelnut shell (5.2 wt% to 10 wt%), sunflower shell (6.1 wt% to 11.5 wt%) and walnut shell (4.8 wt% to 9.1 wt%) were found to increase by increasing temperatures from 377 to 477 °C at 23 MPa and a 10 wt% feedstock concentration for 60 minutes [11]. In another SCWG study, the hydrogen yields of orange peel increased from 0.08 to 0.9 mol/kg biomass as the temperature elevated from 400 to 600 °C at a constant 1:5 biomass to water mass ratio and 23-25 MPa for 45 min [12]. The trend for hydrogen yields from waste cooking oil showed an increase with the rise in temperature from 375 to 675 °C with a maximum yield (4.1 mol/kg biomass) attained at 675 °C with a 25 wt% feed concentration and 23-25 MPa for 30 min [13]. The hydrogen yields of unsorted food waste increased by 85.3% from 2.9 to 5.4 mol/kg biomass with increasing reaction temperature from 420 to 480 °C when the reaction time, feedstock concentration and pressure were kept at 30 min, 5 wt% and 23-28 MPa [14]. The SCWG of fruit pulp showed that hydrogen yields increased approximately 4.5 times (12.2

to 54.1 mol/kg biomass) with an increase in temperature from 400 to 600 °C when the other conditions were kept constant at 2.5 wt% biomass concentration, 40 wt% Ru/C catalyst loading and 25 MPa [15]. By increasing temperature from 380 to 460 °C, the hydrogen yields of almond shell increased by the factor of 1.94 with 10 minutes reaction time, at 1 wt% biomass concentration and 23.5-26.8 MPa [16]. In a recent SCWG literature, the hydrogen yields of food waste were raised from 3.7 to 8 mol/kg biomass by increasing temperature from 420 to 480 °C when the other conditions were kept at 40 minutes reaction time, 8 wt% biomass concentration, 1 wt% catalyst loading of lanthanum promoted Ni/Al_2O_3 and 26-30 MPa [17].

Several SCWG studies have investigated the effect of raising the temperature from subcritical to supercritical conditions on the hydrogen yield. With the rise in temperature from 300 °C (subcritical) to 550 °C (supercritical) in a gasification study, the hydrogen yields of pinecone increased from 0.02 to 0.8 mol/kg biomass at 25 wt% biomass concentration and 21-23 MPa for 30 minutes reaction time [18]. The hydrogen yields during SCWG of pinewood over 45 min increased from 0.2 mol/kg biomass at 300 °C to 0.8 mol/kg biomass at 500 °C at 1:5 biomass to water mass ratio and 23-25 MPa [19]. A huge shift in hydrogen yields was observed from 0.7 to 13.8 mol/kg biomass with the change in temperature from 300 °C to 500 °C for the SCWG of nickel-impregnated sugarcane bagasse at 1:8 biomass to water mass ratio and 23-25 MPa for 50 minutes [20]. Under the same experimental conditions, hydrogen yields rose from 1.6 to 9.5 mol/kg biomass for nickel-impregnated mosambi peels with the shift in operating temperature from 300 to 500 °C. An increase in temperature from 300 to 550 °C resulted in around 10-fold rise in the hydrogen yields of wheat straw from 0.3 to 3 mol/kg biomass at a fixed 20 wt% biomass concentration and 60 minutes reaction time and 21-23 MPa [21]. Hydrogen yields of banana pseudo-stem [22] were raised from 0.7 to 4.2 mol/kg biomass with an increase in temperature from 300 to 600 °C at a constant 1:10 biomass to water mass ratio and 22-25 MPa for 60 minutes. In another study, hydrogen yields of soybean straw were increased from 1 to 3.4 mol/kg biomass with a rise in temperature from 300 to 500 °C at a fixed 1:5 biomass to water mass ratio and 22-25 MPa for 45 minutes [23].

Gasification temperatures also have a significant effect in continuous mode [24][25] e.g. the hydrogen yields of wood sawdust were increased from 13.8 to 18.5 mol/kg biomass with only a modest increase in temperature from 600 °C to 650 °C under the conditions of 2 wt% wood sawdust + 2 wt% CMC as the feedstock

concentration, 30 MPa and 27 s residence time [24]. Continuous SCWG of corn cob [25] increased hydrogen yields sharply from 2.6 to 9.1 mol/kg biomass with the increasing temperature from 550 to 650 °C under the conditions of 25 MPa, 5 wt% corn cob + 2 wt% CMC feedstock concentration, 25 g/min feedstock flow and 127 g/min SCW flow.

SCWG studies using sugarcane bagasse and mosambi peels [20], pinewood [26], waste cooking oil [13] and orange peel [12] have shown that the increase of hydrogen yields with increasing temperature is coupled with a decline in the CO yields and a rise in CO_2 yields which indicates that WGS reaction is promoted at elevated temperatures.

Whilst ionic product mechanisms ($K_w = [H^+][OH^-]$) are promoted in subcritical water (SbCW) and near critical water (NCW), the free-radical mechanisms are more favoured in SCW [27]. Increasing temperature increases the endothermic process of splitting of water to ionic products (H^+ and OH^-) at SbCW and NCW conditions [9]. In contrast, the significant drop in density at supercritical conditions (e.g. 0.1 g/cm^3 around 374 °C) reduces the formation of ionic products (H^+ and OH^-) [28] but creates more hydronium ions (H_3O^+) which, in turn, reduces its pH compared to liquid water [9]. This lowering of pH favours the generation of free radicals, which results in superior solvation of biomass components leading to higher gas yields [9][29]. In addition, low-temperature SCWG leads to hydrolysis reactions (via ionic mechanism) causing bond cleavage and dehydration. On the other hand, high temperature SCWG can result in pyrolysis reaction (via free radical mechanisms) causing decomposition, depolymerization, decarboxylation and deamination of biomass components [13] which increases gas yields.

2.2 The effect of residence time to the gasification efficiency

Residence time (or reaction time) is another variable that directly affects gasification efficiency and specific gas yields. Batch mode SCWG studies usually report minutes to tens of minutes for residence times. In contrast, continuous-mode SCWG studies generally report tens of seconds residence time to complete the gasification process [30][24]. Gasification efficiency and hydrogen yields usually increase with increasing residence time [30].

Batch mode: For some types of biomass, gasification efficiency tends stabilise over time, e.g. 30 minutes [15][31]. For instance, the hydrogen yield of fruit pulp reached a maximum yield at 54.1 mol/kg biomass after 30 min with a 2.5 wt% feedstock concentration at 600 °C and 25 MPa [15]. Longer residence times were not particularly effective in the case of fruit bunches from oil palm [31], where hydrogen yields increased rapidly from 0 to 50 mmol/mL with an increase in reaction time of 0 to 8 minutes but showed only a modest increase (50 to 73 mmol/mL) when the reaction time was extended up to 32 minutes and no significant increase beyond 32 minutes at 380 °C, 24 MPa and 0.3g biomass + 8mL water as the feedstock. Hydrogen can be generated over long periods of time but clearly there is a peak production time depending on the nature of the feedstock itself e.g. the maximum hydrogen yields of 7.3, 4.1 and 4.6 mol/kg of wheat straw, almond shell and walnut shell occurred at 10, 15 and 20 min, respectively when the other conditions were fixed at 1 wt% biomass concentration, 440 °C and 25 MPa [32]. Wheat straw has the highest cellulose and lowest lignin content and was able to generate the highest hydrogen yield with the shortest reaction time [32]. The hydrogen yields of orange peel showed a modest but consistent increase in yield (0.9 mol/kg biomass) at 45 min when compared to the data (0.7 mol/kg biomass) at 15 min when operating at 600 °C, 1:5 biomass to water mass ratio and 23-25 MPa [12]. Hydrogen from pinecone increased by 170% (1.4 versus 0.5 mol/kg biomass) with an increase in residence time from 15 to 60 min when the other conditions were fixed at 550 °C and 23 MPa with 10 wt% feed concentration [18]. The hydrogen yields of unsorted food waste noticeably increased by 20.3% from 5.4 to 6.5 mol/kg biomass as an increase in residence time from 30 to 45 min at a fixed 5 wt% feedstock concentration, 480 °C and 28 MPa [14] with pinewood and wheat straw showing a similar trend [19]. Hydrogen yields from waste cooking oil showed an increase from 0.95 to 5.2 mol/kg biomass with an increase in reaction time from 15 to 60 min under the conditions of a constant 25 wt% feedstock concentration and 675 °C at 23-25 MPa [13]. The respective yields of CO_2 and CH_4 also increased to 1.3 and 3.5 mol/kg biomass at 60 min. CO production, however, does not favour longer reaction times. The decrease in CO yield (0.45 mol/kg biomass) at a longer reaction times parallels an increase in H_2, CO_2 and CH_4 which suggests that WGS reaction and methanation reactions are favoured. This was found to be the case with sugarcane bagasse [33] and wheat straw [21] where longer residence times are required to drive the WGS reaction in order to produce CO_2 and H_2 [34]. However, when the residence times were extended further (beyond 70 mins), methanation

reactions that consume hydrogen become more likely causing a drop of hydrogen yield from its peak value [13][21]. Almond shell and soybean straw also found to show the same trend [16][23].

Continuous mode: Wood sawdust [24] showed a sharp increase in the hydrogen yields (13.5 to 18.5 mol/kg biomass) as the residence time increased from 9 to 46 s with 2 wt% wood sawdust + 2 wt% CMC at 30 MPa and 650 °C. At the same time, the CH_4 yields increased and CO decreased. Similar results were reported for corn cob + CMC [30].

Gas yields are found to increase with longer reaction times due to the dominance of thermal cracking reactions including dehydration, decomposition, decarboxylation and depolymerization [35]. At low reaction times, the efficiency of hydrothermal liquefaction increases, which liquefies the reactive components to generate more stable components such as acetic acid, phenol, and methanol. Conversely, longer reaction times allow gasification reactions and free radical mechanisms to crack these intermediates (e.g. alkylated benzene, acetaldehyde, hydroxyacetone, carboxylic acids and oligomers) to produce gases [13].

2.3 The effect of feedstock concentration/biomass-to-water mass ratio to the gasification efficiency

Feedstock concentration is another parameter (in addition to temperature and residence time) that significantly affects gasification efficiency and hydrogen yield. During SCWG, water has dual roles as both reactant and reaction medium. Reaction pathways include hydrolysis, steam reforming, and WGS reactions, all leading to the main product that is hydrogen [9]. A decrease in water content relative to feedstock concentration effectively suppresses these reactions and therefore potentially inhibits hydrogen yields. Conversely a low feedstock to water ratio can lead to enhanced steam reforming and WGS reactions [18]. Steam reforming reactions allow water to react with a hydrocarbon ($C_xH_yO_z$) to produce hydrogen and CO/CO_2 as end products. Meanwhile, the WGS reaction is a reaction between CO and water vapour releasing hydrogen and CO_2. A higher water to feedstock ratio under SCW conditions should therefore favour both reactions to increase hydrogen production.

Continuous corn cob gasification at 25 MPa and 650 °C [25], showed a hydrogen yield decrease from 12 to 3.8 mol/kg biomass and CO yield increase when the feedstock concentration was increased from 5 wt% to 18 wt%. Increasing the sugarcane bagasse concentration from 0.05 to 0.25 g in 6.5 mL of water also decreased

the hydrogen, CO_2 and CO yields by a factor of 2.8, 3.6 and 1.5, respectively when the other conditions were fixed at 400 °C, 24 MPa and 20 minutes [36]. When the unsorted food waste concentration was increased from 5 wt% to 15 wt%, the hydrogen yields significantly decreased from 7.7 to 3.8 mol/kg biomass at 480 °C and 23-28 MPa and 75 minutes reaction time [14]. Hydrogen yields increased by 32% (0.8 to 1.2 mol/kg biomass) and 117% (1.7 to 3.7 mol/kg biomass) during pinewood and wheat straw gasification, respectively, at 500 °C and 23-25 MPa for 45 minutes when using a 1:10 biomass-to-water mass ratio instead of 1:5 [19]. Hydrogen yields from fruit pulp also showed a similar trend with water:feedstock ratios [15]. The hydrogen yields of nickel-impregnated sugarcane bagasse and nickel-impregnated mosambi peel dropped from 13.8 to 4.9 mol/kg of bagasse and 9.5 to 3.8 mol/kg of peel with the change in biomass-to-water mass ratio from 1:8 to 1:2 under the fixed conditions of 500 °C and 22-25 MPa for 50 minutes [20]. Experiments with wheat straw gasification at 550 °C, 23 MPa and 60 minutes reaction time, reported a drop in hydrogen yields from 3 to 1.1 mol/kg biomass when the feedstock concentration was raised from 20 wt% to 35 wt% [21]. In general, continuous studies report data that indicates that WGS and steam reforming reactions are not favoured by an increasing in feedstock concentrations.

2.4 The effect of pressure to the gasification efficiency

Limited number of SCWG studies with real biomass as the feedstock have investigated the effect of pressure on hydrogen yield. Pressure tends to be fixed whilst altering other variables like temperature and feed concentration. The continuous SCWG of wood sawdust [24] reported that hydrogen yields increased from 15.2 to 17 mol/kg biomass with an increase in pressure from 17 to 30 MPa, alongside a corresponding decrease from CH_4 and CO yields at 650 °C for 27 s residence time when the feedstock concentration was fixed at 2 wt% biomass + 2 wt% CMC. Higher pressures seem to favour the WGS reaction. The hydrogen yields of cotton cocoon shell increased from 5.9 wt% to 12.6 wt% when pressure was increased from 23 to 48 MPa under the fixed conditions at 477 °C and 10 wt% feedstock concentration for 60 minutes [11]. Most reports suggest that increasing pressure has a positive effect on hydrogen yield. Clearly there are issues around CAPEX and OPEX when designing a system to operate safely at higher pressures.

2.5 The effect of biomass composition to the gasification efficiency

As mentioned previously, real biomass will gasify differently, mainly because of the heterogenous nature of the lignocellulosic components [3]. Real biomass contains cellulose, hemicellulose and lignin in different proportions (which generally represents a majority of the biomass) as well as other substances such as alkali salts, sulphur and proteins in smaller quantities [9]. Lignin is a three-dimensional phenyl propane polymer with ester bond links. It holds cellulose and hemicellulose together in a matrix which forms primary cell walls to prevent plant from damages [37]. Cellulose, however, is made of glucose subunits which are linked together with β-1,4-glycosidic bonds that can hydrolyse much more easily into fermentable sugars [37]. It has been reported that hydrolysis of cellulose and hemicellulose proceeds within seconds whereas lignin requires minutes [33].

Compared to cellulose and hemicellulose, which have low thermal devolatilization temperatures of 250-350 °C and 200-300 °C respectively, lignin degrades across a much higher temperature range of 200-500 °C [9]. Lignin has a complex structure and the hydrolysis of lignin into phenolic and conversion of those poly-phenolics into synthesis gas components is unlikely in the absence of a catalyst [32]. The degradation mechanisms of individual biomass components (cellulose or hemicellulose or lignin) under SCWG conditions have been reviewed [9][38], and a review of the interaction effects of binary and tertiary mixtures of biomass compounds has also been reported [38]. To date, several studies have investigated the interaction effect of cellulose-lignin. However, studies including the interaction effects of hemicellulose-lignin and cellulose-hemicellulose-lignin are very limited.

Tables 1, 2 and 3 identifies studies where a lower lignin content, but higher cellulose and hemicellulose content produced higher gases yields and gasification efficiencies [2][37][32][39][20]. In a study, the non-catalytic SCWG of walnut and almond shells with high lignin content (38 wt% and 35 wt% respectively) was found to produce less hydrogen (4.1 and 4.6 mol H_2/kg biomass respectively) when compared to wheat straw (7.3 mol H_2/kg biomass) with higher amount of cellulose (40 wt%) and lower amount of lignin (19 wt%) at 400 °C, 25 MPa, 1 wt% feedstock concentration and 15 minutes reaction time [32]. The authors pointed out that higher hydrogen content in the structure of wheat straw (6.1 wt%) could be another reason for the higher hydrogen yield although the hydrogen of almond shell was only slightly lower (5.4 wt%) whereas the cellulose content

was significantly lower (31 wt%). Another study reported that cotton stalk with a lignin content of 19 wt% was more difficult to gasify than tobacco stalk (13 wt%). The hydrogen yield of cotton stalk was found to be consistently, albeit only slightly, lower than tobacco stalk (e.g. 10.55 mol H_2/kg cotton stalk versus 11.37 mol H_2/kg tobacco stalk at 600 °C, 35-38 MPa, 10 wt% Trona loading and 1 hour) for all reaction temperatures (300-600 °C) and catalyst types (Trona, Borax and Dolomite) investigated [2]. In another example [20], the hydrogen production was found to be significantly lower in mosambi peels (9.5mol H_2/kg biomass) which has higher lignin content (23 wt%) and lower cellulose content (35 wt%) at 500 °C, 22-25 MPa and 1:8 biomass to water mass ratio for 50 minutes. In the same study sugarcane bagasse, with less lignin content (20 wt%) and higher cellulose content (40 wt%), produced a higher hydrogen yield (13.8 mol H_2/kg biomass) [20]. Another paper focussed on hard-shell nuts showed that almond shell > walnut shell > hazelnut shell in terms of hydrogen production at 600 °C and 37 MPa for 1 hour and feedstock concentration of 1.2 g of biomass + 15 mL of water [39]. These results were attributed to the difference in lignin content with hazelnut shell containing the highest lignin content (40 wt%) compared to walnut (35 wt%) and almond (29 wt%). Another batch-mode SCWG study at 440 °C, 1 wt% biomass concentration and 25 MPa and 15 minutes reaction time showed that the order of total gas yields was: canola stalk > wheat straw > rice straw > barley straw > almond shell > walnut shell whereby the lignin content was inversely proportional with total gas yields and cellulose content showed a straight relation with the total gas yields [37].

Not all studies find a correlation between composition and gas yield. The SCWG of cauliflower residue, tomato residue, hazelnut shell, acorn and extracted acorn in a continuous flow system at 8 wt% biomass concentration, 0.8 wt% Trona catalyst loading, 600 °C and 35 MPa [40] showed that lignin content did not correlate to gas yields. The authors concluded that hydrogen yields were enhanced by using continuous flow system compared with batch reactor system even with biomass that contains a higher lignin content. Another batch-mode experimental study [12] revealed that a relatively low hydrogen yield from coconut shell (2.15 mol/kg biomass) at 600 °C, 23-25 MPa, 1:10 biomass to water mass ratio for 45 minutes even though it has the highest lignin content at 46 wt% when compared to aloe vera rind, banana peel, lemon peel, orange peel, pineapple peel and sugarcane bagasse that have lignin contents in the range of 3-32 wt%.

However, most of the studies reveal that (i) the biomass with higher cellulose and hemicellulose content are gasify more readily, (ii) cellulose contributes more to hydrogen yield than hemicellulose and lignin, (iii) the effect of the lignin on the gas yields is less significant at temperatures above 600 °C when using a catalyst - due to the increased ability to gasify lignin. Few studies that investigated the interaction effect between cellulose and lignin reveal that (i) lignin structure gains hydrogen from the cellulose decomposition during the lignin depolymerization which lowers the hydrogen yield and total gas yields [41][42][43][44], (ii) lignin gives a limited contribution to the gas production but reacts in the liquid phase to form other compounds (e.g. tar, solids) [45], (iii) lignin plays an inhibitory action towards hydrogen by interfering with the cellulose degradation mechanism via inhibition of the de-carbonylation reactions and favouring the pathway involving dehydration reactions [43]. It has been reported that hemicellulose also acts as the hydrogen donor for lignin splitting [41] and hemicellulose decomposition produces hydrogen that increases the decomposition rate of lignin [46].

Based on the literature listed in Tables 1 and 2 and 3, sugarcane bagasse, almond shell, corn cob and wheat straw have all shown potential as feedstocks in several SCWG studies. Sugarcane bagasse and almond shell both contain high combined cellulose and hemicellulose contents (71 wt% [20] and 72 wt% [39] for sugarcane bagasse and almond shell, respectively) and produce high hydrogen yields. The hydrogen yield of sugarcane bagasse as high as 23 mol H_2/kg biomass was obtained at 400 °C, 24 MPa, 20 minutes and 0.05 g biomass + 6.5 g water + 0.04 g 20 wt% nickel over CNTs catalyst loading [36]. Hydrogen yields for almond shell were reported to be as high as 11.6 mol H_2/kg biomass under fixed conditions of 460 °C, 10 minutes, 1 wt% biomass feedstock, 27 MPa and 0.4 weight ratio of C. glomerata macroalgae hydrochar catalyst to biomass [16]. Corn cob, which contains 64 wt% combined cellulose and hemicellulose contents and a very low lignin content (3 wt%) [47], produced a hydrogen yield of 15.2 mol H_2/kg biomass at 650 °C, 25 MPa, 40 s and 2 wt% corncob + 1 wt% CMC feedstock concentration [30]. Wheat straw contains 67 wt% cellulose and hemicellulose but with 19 wt% lignin content [32] produced a hydrogen yield of 11.6 mol H_2/kg biomass obtained at 450 °C, 25 MPa, 5 wt% feedstock concentration, 0.2 g Ni/MgO catalyst loading and 20 minutes reaction time [48].

Whilst there have been a number of publications evaluating the effects of cellulose, hemicellulose and lignin contents of different types of real biomass, each publication tends to use different experimental conditions

making direct comparisons difficult. Future studies will also help identify the most promising types of biomass that can generate the highest hydrogen yield for future large scale SCWG processing.

2.6 Non-catalytic SCWG of real biomass

In the past 15 years, 43 papers have investigated the SCWG of real biomass as the feedstock under non-catalytic and catalytic conditions. The significant variables from these papers are summarised in Tables 1, 2 and 3 including biomass composition (cellulose, hemicellulose and lignin), type of reactor used, catalyst type and catalyst loading, operating conditions, hydrogen yield and char formation. Most of the papers related to catalytic SCWG with only few papers focussing on non-catalytic SCWG. As the desired product of SCWG is hydrogen, the WGS reaction should be dominant and methanation reactions should be minimised. This can be achieved by treating feedstocks at high temperature (600 °C or above) or by adding a catalyst in the gasification process. Under non-catalytic conditions, it has been reported that complete gasification is normally only achieved at high reaction temperatures above 600 °C. For instance, relatively high hydrogen yields (12 to 18.7 mol H_2/kg biomass) were reported in the studies of non-catalytic continuous SCWG of wood sawdust and corncob at reaction temperature of 650 °C and short residence time (40 to 46 s) [30][24][25]. Other non-catalytic SCWG studies conducted below 600 °C (380 to 500 °C) reported low hydrogen yields (1.3 to 7.3 mol H_2/kg biomass) in a batch-mode reactor with long reaction times of 10 to 120 minutes [32][49][50][51] . However, operation at high temperatures and high pressures necessitate higher CAPEX and OPEX. It is therefore more desirable to consider catalytic SCWG processes that can achieve higher hydrogen yields at temperatures lower than 600 °C.

2.7 Catalytic SCWG of real biomass

Catalysts play an important role in the efficient production of hydrogen during SCWG, not least because SCWG reactions have high activation energies [52]. Catalysts can significantly improve the conversion of biomass at lower temperatures which, in turn, reduces the capital and operating costs of this process [29]. The choice of catalyst is key to this reduction in OPEX and CAPEX [48]. Many researchers appear to investigate catalyst type as well as the catalyst loading, reaction environment, process parameters, and reactor configuration [5][6][7][8][9][10]. A variety of both homogeneous and heterogeneous catalysts have been tested in SCWG of real biomass with the aim of selectively enhancing hydrogen gas yields whilst lowering

reaction temperature. Most of the catalysts were shown to improve hydrogen and carbon dioxide yields by lowering carbon monoxide yields through the WGS reaction [2]. The physical characteristics of these heterogeneous catalysts are summarised in Table 4.

2.7.1 Homogeneous catalysts

Alkali catalysts (e.g. $Ca(OH)_2$, KOH, $KHCO_3$, K_2CO_3, LiOH, NaOH, NaCl, $NaHCO_3$, Na_2CO_3, $ZnCl_2$) are common homogeneous catalysts that can promote hydrogen production by accelerating the WGS reaction [15]. Alkali catalysts reduce the starting temperature required for cellulose degradation and accelerate WGS reaction resulting in higher yield for hydrogen and CO_2 as well as lower yield for CO [26]. Viable catalysts catalyse the breakage of C−C, C−O, C−H, and O−H bonds to yield a hydrogen rich gas mixture [20]. Most investigations into the use of homogeneous catalysts during SCWG were performed in batch mode at temperatures below 600 °C (i.e. 400 - 500 °C) [47][52][53][18][14][54][23]. In those studies, hydrogen yields in the range of 1.8 to 12.7 mol/kg biomass were reported, which were higher than the range of hydrogen yields obtained from the equivalent non-catalytic SCWG (1.3 to 7.3 mol H_2/kg biomass). Whilst the reduction in operating temperature is beneficial, the recovery of the homogeneous catalyst is difficult to achieve, thus creating additional cost for the ongoing addition of fresh catalyst and the liquid waste containing alkali catalyst generated after the SCWG is difficult to treat [9][55]. These drawbacks have led most researchers to focus on the use of heterogeneous catalysts in order to achieve similar catalytic activity and high selectivity towards hydrogen production.

2.7.2 Heterogeneous catalysts – metal-based with support material

Most SCWG studies using metal-based heterogeneous catalysts were conducted in batch mode. Researchers reported hydrogen yields in the range of 2 to 23 mol/kg biomass with operating temperatures between 400 and 550 °C, [33][20][36][47][52][26][53][56][19][21][16][17]. Operating temperatures higher than 600 °C (600 to 675 °C) show increased hydrogen yields in the range of 2 to 55 mol/kg biomass [52][15][13][22]. It is difficult to make a direct comparison with homogeneous catalytic studies (that do report lower values of 1.8 to 12.7 mol/kg biomass) because of the use of different biomass types and different experimental conditions.

2.7.2.1 Nickel-based versus ruthenium-based catalysts

Metal-based heterogeneous catalysts commonly use nickel and ruthenium due to their ability to catalyze C–C bond breaking and promotional effect on the WGS reaction which increases the hydrogen yield and carbon gasification [55]. Some of the SCWG studies, either with model compound [52] or real biomass [13] as the feedstock, have shown ruthenium to be marginally more active than nickel e.g. waste cooking oil generated a hydrogen yield 10.2 mol/kg biomass with Ru/Al_2O_3 and 9.3 mol/kg biomass with $Ni/Si\text{-}Al_2O_3$, both at 5 wt% catalyst loading [13]. By referring to Table 4, ruthenium has been shown to produce a higher metal dispersion and BET surface area compared to other catalysts (such as nickel) due to a lower ruthenium metal loading (1.5 to 5 wt%) compared to the nickel metal loading (5 to 20 wt%) on the support [52][57]. In one case a 5 wt% of ruthenium loading on Al_2O_3 provided an 8.7% metal dispersion and 226 m^2/g total surface area, however a 20 wt% nickel loading on Al_2O_3 only provided 1.7% metal dispersion and 195 m^2/g surface area when using the same synthesis method [52]. Elsewhere [57], a 5 wt% of ruthenium loaded on activated carbon (AC) and $\gamma\text{-}Al_2O_3$ also provided higher BET surface area and higher metal dispersion than the 5 wt% of nickel loading on $\alpha\text{-}Al_2O_3$. In addition, ruthenium-based support catalysts with higher BET surface area and high metal dispersions [52] and [57] did not lead to higher hydrogen yield than equivalent nickel-based support catalysts. Based on these two results, no dependency of hydrogen yield on surface area and metal dispersion is observed. The optimisation of a catalyst is complex, and not determined by just the metal, the total surface area, the wt% loading or % metal dispersion. High temperature processes, such as SCWG, create diffusion limited reactions and this can mean that micropores (that provide significant surface areas on some supports) and even mesopores are less relevant. Even if ruthenium was a superior catalyst, a simple techno-economic analysis would indicate that nickel would be the preferred option due to its relatively low cost compared to ruthenium [53]. This explains why, as seen in Table 4, nickel is the most common catalyst, followed by ruthenium-based catalysts with smaller % loadings.

2.7.2.2 Nickel-based versus cobalt (Co)-based, copper (Cu)-based and iron (Fe)-based catalysts

A study related to the SCWG of liquefied switchgrass biocrude showed that Ni/TiO_2 and Ni/ZrO_2 catalysts could generate higher hydrogen yields when compared to Co/TiO_2 and Co/ZrO_2 catalysts under the same experimental conditions [58]. A more recent study related to the SCWG of wheat straw demonstrated that the order of catalytic activity for hydrogen yield is Ni/MgO > Fe/MgO > Cu/MgO under the same experimental

conditions [48]. Nickel is known to promote key reactions including the WGS, methanation and hydrogenation all of which help to produce hydrogen and eliminate CO during SCWG [47]. The use of nickel catalyst in SCWG is therefore expected to lead to higher yields of gas products, especially hydrogen and CH_4.

However, hydrothermal instability, susceptibility to sintering, fouling by tar-forming products or carbon deposition all result in a lower selectivity and stability of nickel [9][59][60]. These issues are significant challenges for Ni-based catalyst development. Some studies proposed that a suitable catalyst support/promoter combination could address these problems. Table 3 has shown that tailoring the catalyst support materials is an alternative way to increase the catalytic activity and its stability and gas yields. Potential support compounds that have been investigated in SCWG of real biomass include activated carbon (AC), zirconium dioxide (ZrO_2), titanium dioxide (TiO_2), aluminum oxide (α-Al_2O_3), alumina (except α-Al_2O_3), magnesium oxide (MgO), zinc oxide (ZnO), calcium oxide (CaO) and carbon nanotubes (CNTs).

2.7.2.3 Activated carbon as the support material

Activated carbon generally has a surface area above 1500 m^2/g [61] and can act as a catalyst or catalyst support during hydrothermal gasification with the additional benefits that it does not 'pollute' to the reaction system [9]. The use of AC as a catalyst during SCWG reactions is reported to be ineffective unless operation at higher temperature (e.g. > 600 °C) [7]. In addition, AC appears to deactivate after a few hours [9]. However, AC can be successfully used as a catalyst support across a wider range of temperatures. For example, the hydrogen yield was enhanced by 2.8 times (compared to non-catalytic operation) by using Ru/AC in the SCWG of sugarcane bagasse at 400 °C [33]. In a separate SCWG study, birchwood bark was gasified at 380 °C using Ru/AC as the catalyst and the hydrogen yield was enhanced by 5.9 times [57]. SCWG of fruit pulp using Ru/AC as the catalyst showed that the hydrogen yield was enhanced by 2.5 times at 600 °C [15]. Ni/AC gasification of model compounds (such as glucose) [62][63] have also been investigated, however its application in SCWG of real biomass has not been reported yet. Furthermore, there is little information regarding the stability and activity of Ru/AC and Ni/AC during extended operation.

2.7.2.4 Carbon nanotubes as the support material

Carbon nanotubes are a promising support material with a high surface area, unique electronic properties and chemical inertness, thermal stability and high mechanical strength. In a SCWG study using sugarcane bagasse [36], CNTs acted as a catalyst increased the hydrogen yield by a factor of 1.6 to 1.9, depending on %CNT loading, compared to the noncatalytic experiment. The results also showed that CNTs could be used as the support material for nickel (Ni/CNT), enhancing the hydrogen yield by a factor of 3 to 5.8 depending on the amount of nickel metal loading on the CNTs.

2.7.2.5 Metal-oxides as the support materials

To date, there are limited studies that have investigated and compared the efficiency and stability of different supporting materials for SCWG with real biomass as a feedstock. Hence, some studies with model compounds were referred here. During the catalytic SCWG of lignin at temperatures below 650 °C, it was observed that using different supports impacted the activity of nickel-based catalysts in the following order; Ni/Al_2O_3 > Ni/TiO_2 > Ni/AC > Ni/ZrO_2 > Ni/MgO [64]. Osada et al [65] reported that the stabilities of different Ru-supported catalysts as; Ru/TiO_2 > $Ru/\gamma\text{-}Al_2O_3$ > Ru/AC during the SCWG of lignin at 400 °C with 180 minutes reaction time i.e. Ru/TiO_2 maintained its high gasification activity for three subsequent cycles whereas Ru/AC lost its activity after the first run due to the decrease in its surface area. Although $Ru/\gamma\text{-}Al_2O_3$ showed good catalytic performance at the initial stage, its activity gradually reduced during repeat cycles due to its structural transition from gamma-state to alpha phase and dissolution of ruthenium in SCW. In another work, the potential to reuse the $Ru/\alpha\text{-}Al_2O_3$ catalyst twice in a batch system at 550 °C for 10 minutes reaction time was tested in SCWG of glucose [66]. The results suggested an increasing level of hydrogen production, while methane production showed a decreasing trend. However, it is unclear why changes in the selectivities of product gases with repeated used of the $Ru/\alpha\text{-}Al_2O_3$ were observed.

In a study related to the SCWG of sugarcane bagasse at 400 °C for 15 min reaction time, the application of Ru/TiO_2 generated higher hydrogen yields than Ru/AC (3.2 versus 2.3 mol H_2/kg biomass) [33]. The authors also studied the stability of the Ru/AC catalysts by repetitive use of the same catalyst over five cycles in the SCWG of sugarcane bagasse. The gas yield after five repeat experiments stabilised at 71.5% due to the decrease in surface area of the carbon support. Possible explanations for the decrease of surface area include a breakdown of pore structure of the carbon support and/or the pores were fouled by small amounts of

carbonaceous products during gasification. The results indicate that the ruthenium metal in the pores would not work for gasification after repetitive use; hence, gasification efficiency decreased gradually.

In another publication, continuous SCWG of switchgrass biocrude at 600 °C revealed charring of all catalysts (Ru/TiO_2, Ru/ZrO_2, Ni/TiO_2, Ni/ZrO_2, Co/TiO_2, Co/ZrO_2) at the entrance of the reactor as the biocrude was heated and all support materials suffered significant surface area loss due to sintering after 2 hours of operation [58]. A more recent study about the SCWG of wheat straw at 450 °C over a 20 min reaction time showed that the order of nickel catalysts' activity with different supports in terms of hydrogen yield was Ni/MgO > Ni/ZnO > Ni/Al_2O_3 > Ni/ZrO_2 under the same experimental conditions [48]. In that study, the activity and stability of Ni/MgO were compared for three consecutive runs. The hydrogen yield was 11.6 mol/kg biomass when the fresh Ni/MgO catalyst was used, decreasing to 7.4 mol/kg when used again, dropping to 5 mol/kg when used a third time. It was found that the severe deactivation of Ni/MgO catalysts happened after the gasification reaction was caused by catalyst coking, adsorbing of substances leading to the poisoning of the catalyst, sintering and wrapping of the active component. In essence three of the four most common routes to deactivation were found to be occurring (apart from loss of active species). The authors explained that the long term performance of Ni/MgO catalysts not only depends on the dispersion of metal in the support but also the selection of support material itself.

A recent study investigated the stabilities of catalysts Ni/Al_2O_3 and lanthanum (La) promoted Ni/Al_2O_3 during the SCWG of food waste [17]. The catalytic performance of La promoted Ni/Al_2O_3 in hydrogen production dropped by 31% and 65% in second and third runs, respectively. The decrease in catalytic performance was more significant with Ni/Al_2O_3 with a 87% decrease observed during the third run. Most results indicate some loss of catalytic activity when the catalyst is repeatedly used due to the deactivation of the catalyst by carbon deposition (fouling) and the loss of active species caused by a cracking of catalyst surface (observed using SEM analysis). In addition, sintering and migration is also highly likely as a result of the extreme temperatures and pressures required for SCWG. The use of Lanthanum promoter increased the lifespan of the catalyst by improving the resistance to carbon deposition on catalyst surface.

In general, the literature shows that the metal supported catalysts improve the hydrogen yield particularly with single use batch experiments. However, the activity and stability of the catalyst is not guaranteed particularly with repeat or continuous use.

2.7.3 Heterogeneous catalysts – natural mineral-based

Natural mineral catalysts such as Trona [89.2 wt% $Na_3(CO_3)(HCO_3)\cdot 2H_2O$], Borax [81.7 wt% $Na_2B_4O_7\cdot 10H_2O$], Dolomite [31.2 wt% $CaMg(CO_3)_2$] and olivine [$(Mg, Fe)_2SiO_4$] have been shown to increase the hydrogen yields during SCWG [2][39][47][26][40]. Mineral catalysts have the advantages of being low cost, ready availability and do not need to be recovered. A study related to the SCWG of peanut shell showed that olivine and dolomite increased hydrogen yields by 46.2% and 37.8%, respectively, compared to catalyst free operation [53]. The results revealed that although their catalytic effects were not as significant as KOH and $Ca(OH)_2$ but they were still higher than that of Na_2CO_3 and NaOH. In another paper, dolomite was found to be less effective when compared to KOH and $Ni/CeO_2/Al_2O_3$ in the SCWG of pinewood [26]. The effectiveness for three different natural mineral catalysts in the SCWG of cotton and tobacco stalks [2], hazelnut shell and walnut shell and almond shell [39] can be classified as being Trona > Borax > Dolomite. A SCWG study using cotton stalk and corncob showed that the gasification activity of Trona was similar to that of commercial alkali catalyst (K_2CO_3) and higher than red mud and Raney nickel. Another study also found that Trona was as effective as K_2CO_3 in the SCWG of cauliflower residue, hazelnut shell, acorn and extracted acorn suggesting that Trona was a more economical catalyst than commercial alkaline catalysts.

2.7.4 Heterogeneous catalysts – others

Apart from metal-on-support and mineral-based catalysts, there are other heterogeneous catalysts that have shown positive catalytic effects. One particular SCWG study established that red mud showed catalytic activity during the production of hydrogen from the sunflower stalk, corncob and vegetable-tanned leather waste [47]. The hydrogen yield in the presence of red mud was comparable to Raney Ni under the same experimental conditions and the yield was enhanced by 119%, when compared to non-catalytic conditions. Red mud (specific surface area: 16 m^2/g) is a by-product of the electrochemical process used in aluminium

production and contains mainly Fe_2O_3 (37.7%), Al_2O_3 (17.3%), SiO_2 (17.1%), TiO_2 (4.8%), Na_2O (7.1%) and CaO (4.5%).

In a recent study, hydrochar (which is the solid residue that remains after the SCWG of Cladophora glomerata (C. glomerata) macroalgae or wheat straw) was employed as the catalyst to produce hydrogen from almond shell [16]. Hydrogen yields were enhanced by 37% and 47% in the presence of wheat straw and C. glomerate hydrochars, respectively, compared to noncatalytic experiments. Both wheat straw and macroalgae hydrochars contain alkali and alkaline metals (Ca, K, Mg and Na) with a high surface area (see Table 4). The cracking of the biopolymers in the almond shell also promoted the WGS reaction in the gas phase which, in turn, elevated the hydrogen production and total gas yields.

2.7.5 Impregnation of nanocatalyst into the biomass feedstock

More recently, the direct integration of nanocatalysts into biomass has generated some promising results [20][19][22]. In order to work successfully, the biomass must have the capability to adsorb/integrate metal ions from the solution into the lignocellulosic matrix. In addition the metal loading and pH of the metal aqueous solution is important. For instance, a study that impregnated the nickel nanocatalyst into pinewood and wheat straw and the gasification of nickel-impregnated biomass showed considerably higher hydrogen yields with an increase of 155% and 60% for pinewood and wheat straw respectively, when compared to noncatalytic gasification [19]. In another study sugarcane bagasse and mosambi peel [20], impregnated with a nickel salt solution (resulting in to the formation of 10nm $NiO/Ni(OH)_2$) enhanced the hydrogen yield and overall gas yields. Higher nickel concentrations were observed in the bagasse compared to mosambi peels (1.1 versus 0.4 mol/kg biomass) which was attributed to the high levels of cellulose and hemicellulose in the bagasse which provide more active surface sites for the uptake of the nickel species. The higher metal (nickel) loading in bagasse led to higher hydrogen yield (13.8 mol/kg biomass) over mosambi peel (9.5 mol/kg biomass). A recent literature about SCWG of banana pseudo-stem demonstrated that the highest hydrogen yield at 11.1 mol/kg biomass was obtained with nickel-impregnated biomass when compared to ruthenium-impregnated (8.8 mol/kg biomass), iron-impregnated (8 mol/kg biomass) and raw biomass (4.2 mol/kg biomass) [22].

It is clear that the optimization of the catalyst loading and process parameters is critical in determining the optimum process conditions required to maximise hydrogen production at temperatures below 600 °C. There are still gaps in the knowledge required to make low temperature gasification possible through the use of catalysts. Firstly, the performance of promising catalysts (identified in the literature) need to be compared under identical experimental and reaction conditions. Secondly, the performance of these catalysts need to be evaluated using real biomass materials rather than model compounds.

3. Initial Economic Considerations for Catalytic SCWG at 400 °C and Non-catalytic SCWG at 600 °C

A few of the more recent batch-mode SCWG studies using real biomass as the feedstock (e.g. sugarcane bagasse [33][36][56], birchwood bark [57], peanut shell [53], empty palm fruit bunches [55]) have focused on the use of heterogeneous catalysts (particularly metal-based with support material) to allow lower temperatures to be used (e.g. 380 and 400 °C). Reasonable hydrogen yields, in the range of 2.3 to 46 mol H_2/kg biomass, were reported in these studies.

It is logical that running lower temperature SCWG with catalyst (Scenario 1) is more viable than high temperature SCWG without a catalyst (Scenario 2). Unfortunately there is not a lot of literature that make the direct comparison of the gasification efficiencies of catalytic and non-catalytic SCWG conditions either in batch or continuous mode. Economic analysis of SCWG with model or real biomass feedstocks has not been reported so far either.

We have carried out an initial simulation and economic study on the continuous-mode SCWG process with wheat straw as a feedstock using Aspen Plus V11 in order to compare the CAPEX and OPEX of catalytic SCWG at 400 °C and non-catalytic SCWG at 600 °C at 22.1 MPa. It is assumed that Scenario 1 at 400 °C with catalyst achieves the similar gasification efficiency as Scenario 2 at 600 °C and the products contain H_2, CH_4, CO, CO_2, H_2O and ash [67]. Biomass is modelled by using its proximate and ultimate analysis data listed in Table 5. The SCWG reactor is modelled by combining the RYield and RGIBBS reactors in Aspen Plus. Biomass is initially defined as non-conventional solid and the RYield block with FORTRAN subroutine is used to convert the solid biomass into its compositional elements, and then the RGIBBS reactor is used to predict the equilibrium product composition from the SCWG process by applying direct minimization of Gibbs free energy [23][68][67][69]. Peng Robinson with Boston Mathias mixing rules (PR-BM) is used in

calculating the product yields from the SCWG reactor. It has been reported that PR-BM property method produced the closest value with the experimental data [68] and employed in other SCWG modelling studies [68][67][69]. The feedstock stream (20,000 kg/h) contained 5 wt% wheat straw (1000 kg biomass/h) [70]. With reference to a batch-mode SCWG study of wheat straw that investigated the activity of nickel on different supports [48] - a 10 wt% Ni/MgO was selected as the catalyst for Scenario 1.

Metal-based catalysts are commonly prepared by impregnation method. Supercritical hydrothermal synthesis (SCWHS) is an emerging technology which takes advantage of the tuneable chemical and physical properties of supercritical water to produce metal oxide nanocatalysts by rapid nucleation [71]. A recent study reported the feasibility of combining supercritical water oxidation with 'in-situ' hydrothermal synthesis of nanocatalysts and the initial economic analysis showed the financial viability of this combined process [72]. It is postulated that a similar idea can be applied here by combining the modelling of SCWG of wheat straw with 'in-situ' hydrothermal formation of the Ni/MgO nanocatalyst to produce a combined process of SCWG and Ni/MgO nanocatalyst production which can speed up the gasification rate at 400 °C via enhanced catalytic activity. Plugging and reactor corrosion issues are not considered in this preliminary economic study because it is expected that the application of co-current reactor has the potential to minimise reactor corrosion [73] and the design of fast heating rate of the feedstock could also minimise the formation of char [7][74]. The details of the co-current reactor configuration are presented in Section 4.3. The close association of fast heating of cold feedstock flow with its potential to minimise char formation, plugging and corrosion is discussed in detail in Section 4.2.

Figure 1 shows the Aspen Plus simulated SCWG process. Mass balances are presented in Tables 6 and 7 and the costs for different materials are listed in Table 8. The biomass solution is not heated and enters at the bottom end of the reactor. The water is pre-heated in a heat exchanger with the heat recovered from the reactor effluent and then heated to the supercritical condition (400 or 600 °C, 22.1 MPa) by a gas-fired boiler using natural gas. For the catalytic SCWG at 400 °C, the metal salts (nickel nitrate hexahydrate and magnesium nitrate hexahydrate) are continuously fed into the reactor with the stream of biomass solution. It is assumed that the Ni/MgO catalyst that enhances the gasification efficiency at 400 °C is being constantly generated 'in-

situ' and the used catalyst is constantly removed from the reactor with the reactor effluent. Catalyst recovery for regeneration and reuse in consecutive runs is not considered here.

Table 9 clearly shows that non-catalytic SCWG at 600 °C contributes to higher utility, capital and operating costs when compared to catalytic SCWG at 400 °C. Operation at higher temperature (600 °C) requires the selection of high-grade heat-resistant and anti-corrosive tubing and fittings (e.g. Inconel 625) which is more costly when compared to lower temperature fittings (e.g. SS316). In addition, the heating costs for non-catalytic SCWG at 600 °C is obviously significantly higher than the catalytic SCWG at 400 °C. The electricity requirements of the pumps are essentially the same for both scenarios.

This preliminary economic analysis demonstrates that the catalytic SCWG process at 400 °C is theoretically more economically feasible than non-catalytic SCWG process at 600 °C. Moving forwards, experimental work would need to develop effective catalyst(s) that enable low temperature SCWG with a range of potential biomass feedstocks e.g. sugarcane bagasse, almond shell, corn cob and wheat straw.

4. SCWG Reactors- Development and Challenges

4.1 Batch versus continuous reactors

Batch and continuous reactors have both been used in laboratory scale SCWG studies of real biomass. Tables 1, 2 and 3 highlights where different types of batch reactors have been used including autoclaves, micro-quartz capillary reactors and tubular reactors. Continuous reactors have tended to be tubular reactors or fluidized bed reactors. Batch reactors tended to be autoclaves with a volume of between a few millilitres to 1 L. With batch processing, the components of biomass and water (with or without catalyst) were sealed inside the autoclave reactor agitated with the help of a stirrer. Batch reactors are normally confined to fundamental studies and therefore highly suitable for investigating the gasification efficiency of a real biomass. Fixed volume cells can allow the effects of some operating parameters to be isolated (e.g. temperature, pressure, reaction time and biomass concentration), as well as the influence of different catalysts and catalyst loading. Continuous flow reactors can make isolation of operating variables more difficult to separate [75].

It is little evidence in the literature to suggest that the SCWG process could be scaled up to industrial scale using a batch reactor. However, challenges with continuous flow reactors remain around how to maximise the

hydrogen production efficiency whilst minimising char formation, reactor corrosion and plugging [25][58][40]. These studies will give an insight into the feasibility to scale-up from laboratory scale towards pilot scale. Char formation can arise from the slow heating rate of the feedstock and incomplete gasification [7][76]. Plugging is generally a result of slow flow rates or poor mixing of a multiphase flow containing solids and the precipitation of salts at high supercritical temperature in a low density, high temperature flow regime [77]. Reactor corrosion is also a major issue caused by presence of halides and other corrosive species that actively breakdown the reactor walls. The potential to overcome these issues is discussed in the following sections.

4.2 Char formation and plugging

Char formation is a key problem during the SCWG of real biomass because it causes plugging in the reactor [10]. Plugging can also accelerate reactor corrosion rate and catalyst inactivation rate, and reduce heat transfer coefficient of reactor wall [78]. When the reactor becomes plugged, it has to be shut down, cleaned and then restarted, which increases running costs which would create issues around the viability of commercial operation. Most of the SCWG studies listed in Tables 1, 2 and 3 that use actual biomass as the feedstock report the observation of char formation in the reactor after the experiment. Unfortunately there are only limited studies that attempt to quantify char yield [47][49][50][26][19]. In general char yield is not quantified even though char was found in the reactor after the experiment [2][4][12][18][24][31][32][33][39][20][52][15][53][16]. More information is needed about the quantification of char yield, the factors and components that contribute to the char formation, and the mechanism of char formation during the reaction.

For batch-mode SCWG studies, the role of the slow heating rate in increasing char formation has been reported to be significant [7]. Fast heating [74] has been proposed and investigated in some studies in order to reduce or minimise char formation. Rapid heating has also been shown to increase gasification efficiency as well as hydrogen yield. Chuntanapum and Matsumura recently clarified the role of 5-(hydroxymethyl)furfural (5-HMF) in tarry materials formation. Their study found that polyaromatic char formation occurred only in the sub-critical conditions, and resulted from the polymerization of 5-HMF and its aromatic degradation products [79]. The intermediate compound 5-HMF was observed to form high molecular weight char material in sub-

critical water at 25 MPa and 350 °C, but was completely gasified in supercritical water at 450 °C. In another work, Kruse et al. found that char was generated with slower heating rates [76]. The authors explained that low heating rate increases the time that the feedstock spends at sub-critical temperatures before reaching supercritical temperatures and this leads to formation of furfurals or other unsaturated compounds that can polymerize to form high molecular weight char [80]. Matsumura's group also investigated SCWG at different heating rates and found that a heating rate of 10^2-10^3 °C/min was necessary to inhibit coke/char formation [81].

Many of the batch-mode SCWG studies listed in Tables 1, 2 and 3 used low heating rates (~10 °C/min) and report the formation of char during the reaction [2][31][39][47][49][52][26][53][55][21][82][54]. In those studies, the biomass and water mixture were loaded into the reactor (autoclave / micro-quartz capillary reactor / tubular reactor) at room temperature and then heated to supercritical conditions at heating rates of 3 to 30 °C/min. This would therefore require longer heating times and, more importantly longer times at near-critical conditions which leads to the formation and deposition of char around the entrance of the reactor [58].

Char formation has also been observed and reported in continuous tubular reactors which can block the flow over time. Examples include char formation in the continuous-mode SCWG studies of wood sawdust [24], cauliflower residue, acorn, tomatoes residues, extracted acorn and hazelnut shell [40], and switchgrass biocrude [58].

Blocking is not inevitable. In a "VERENA" pilot-scale continuous-mode SCWG process (Figure 2) with maize silage and corn silage/ethanol as the feedstocks [83], char formation and plugging was avoided by adopting two strategies: (i) the biomass feedstock was heated up to subcritical temperature before it entered the reactor and then the feedstock was heated to supercritical temperature rapidly after it was mixed with SCW in the reactor, (ii) due to the flow direction and gravity of the down flow tubular reactor, the settled salts were accumulated in the lowest part of the reactor and separated from the reaction system by a brine removal system.

A continuous-mode fluidized bed SCWG reactor was proposed to overcome the plugging problem (commonly encountered with tubular reactors) using corn cob as the biomass [25]. The results showed that char formation and reactor plugging was not evident after 5 hours continuous operation, even with a relatively high feedstock concentration (18 wt%). The TU Delft/Gensos semi-pilot scale study that incorporated a fluidized bed reactor

(Figure 3) [84] reported that the highest carbon gasification efficiency at 73.9% was obtained at 600 °C reactor temperature and a feed flow rate of 24.5 kg/h whilst using dry starch concentration of 4.4 wt % as the feedstock. Whilst no blocking was observed, small quantities of char (2.3 wt% at highest) and oil production (10.4 wt% at highest) were found in the pipework after shut down. Existing literature indicates that fluidized bed reactors may avoid reactor plugging, but these studies are still at the design stage. High energy demands, high operating costs and design complexity are some of the challenges facing fluidized bed configurations, and these will need to be addressed [6].

In summary, char formation is closely associated with the way that the biomass feedstock is mixed with the SCW flow. To date, two different mixing approaches have been discussed: (i) mixing water and biomass feedstock at room temperature before heating the slurry to supercritical conditions (Figure 4), and (ii) injecting a biomass feedstock slurry at room temperature into SCW (Figure 5). The premixing approach clearly describes all the batch-mode studies listed in Tables 1, 2 and 3 and the continuous-mode SCWG study of clover grass [84][85]. Heating rates are slow giving rise to char formation in the preheater and reactor. In addition, the impact of supercritical conditions is less clear when it is likely that catalytic gasification reactions will have started during the heating process, making it hard to accurately define the reaction times. Nevertheless, the premixing strategy has been widely used for catalytic SCWG experiments and some papers overlook the issue of inaccurate batch reaction time/temperature calculations. Most of the continuous-mode SCWG studies compiled in this review mix a biomass slurry with a preheated SCW flow [24][25][58][40][83]. This can be assumed to rapidly heat the feedstock to supercritical temperature, making it easier to calculate a definitive reaction time. This mixing strategy also reduces char formation considerably whilst allowing for more accurate calculations of residence time for chemical kinetic studies.

It has been reported that higher feedstock concentrations can cause plugging more easily, which is why low feedstock concentrations tend to be used [5]. Further investigation is required, however, to fully understand the effects of feedstock concentration on char formation and plugging. The SCWG process needs pressure to be monitored in the cold zones, preferably before the preheaters in order to operate safely. A sudden rise in pressure would indicate a clog downstream due to plugging. The installation of rupture discs or pressure relief valves on the front end of the reactor is recommended to avoid system failure in the case of over-pressurization.

The absence of a significant pressure drop between the inlet and outlet of reactor, after several hours of continuous operation, would indicate that reactor plugging was not taking place [84]. To overcome the clogging of the back-pressure valve, a particulate filter can be placed before the back pressure relief valve in order to remove entrained precipitated salts and char.

4.3 Reactor corrosion

Another challenge encountered during SCWG is corrosion which can shorten operating lifetimes, and/or lead to a failure of process equipment as well as lower gasification efficiencies [86]. Reactor corrosion is mainly caused by chemical attack from halides present in the biomass or by galvanic corrosion catalysed by the deposition of precipitated salts or metal oxides on the walls of the reactor itself [77]. Salts, either added as catalysts or naturally present in biomass feedstocks, have low solubility in SCW (usually lower than 100 mg/L) and so readily form solids [3][78]. Alkali metal salts are 'tacky' at temperatures above 300 °C and tend to stick to reactor surfaces where they first experience supercritical conditions. In a SCWG study using corn silage, the authors reported significant levels of corrosion and a thinning of the reactor walls during operation [87]. To date, there are few reports that have looked at ways to mitigate against reactor corrosion. Pinkard and co-workers describe four primary routes to avoid corrosion [10] which include:

(i) Flow control (through reactor optimisation) that prevents corrosive species from interacting with the reactor surface
(ii) Use of a sacrificial sleeve that forms a corrosion-resistant barrier
(iii) Selecting corrosion resistant materials
(iv) Optimising operating conditions to reduce corrosion

Whilst SCWG studies are relatively scarce, there are extensive studies around reactor corrosion during supercritical water oxidation (SCWO). SCWO and SCWG are similar because they both require supercritical conditions, and both use organic compounds as the feedstock and also experience the same reactor problems (char formation and reactor corrosion). Some authors have found that reactor corrosion can be largely avoided by using reactors that control flow characteristics e.g. the reverse-flow tubular reactor and transpiring wall reactor (TWR) [78]. The reverse-flow tubular reactor was employed in the SCWG pilot plant named "VERENA" (Figure 2) with a slurry of corn silage and ethanol as the feedstocks for a total throughput of 100

kg/hr with maximum 20 wt% dry biomass loading [83]. Inside the reactor, the salts are transported downwards by gravitation and separated using a brine removal system. This reactor design could largely prevent the salts from interacting with the reactor surface and thus minimise reactor corrosion.

Marrone and Hong [86] stated that TWRs have limited use for SCWG due to adverse effect of the dilution flow (which is part of the TWR design, Figure 6(a)) on the energy balance of the process. In addition, solids precipitation in TWR (Figure 6(b)) was found to be prevalent [73]. A new co-current reactor configuration (designed for SCWO) (Figure 7) [73] could potentially be applied to SCWG in order to minimise reactor corrosion. The reactor volume is divided into two main zones which are 'reaction zone' and the 'wall zone' whereby the SCW flows in the outer pipe (wall zone) co-currently with the cold feedstock flowing upwards from the inner pipe, the mixing between SCW flow and feedstock flow and reaction occur at reaction zone with the resultant mixture carried upwards towards the outlet of the reactor. This reactor design avoids proximity between the corrosive species and the reactor walls whilst providing sufficient mixing between the feedstock and SCW in the middle of reactor.

Corrosion-resistant reactor wall materials such as Inconel-625, Hastelloy C-276 and SS-316, that have proven to be applicable during SCWO, are used for SCWG because of their ability to operate at high temperatures and pressures. However, these alloy materials are expensive which increases the CAPEX of the SCWG process [88]. The use of ceramic materials (such as alumina) to protect the reactor surface from corrosion was investigated during the SCWG of real biomass (beech sawdust and malt spent grains) as well as model compounds (glucose and a glucose/phenol mixture) at 400 °C and 30 MPa for 16 hours with a stainless steel autoclave reactor with an inner alumina (Al_2O_3) sleeve [88]. Scanning electron microscopy (SEM) images of the sleeve post reaction showed that very small spheres of carbonaceous products were present and covered the surface almost uniformly (Figure 8(b) and 8(d)), however the carbon layer got detached from some points on the surface after washing the surface with acetone showing that the surface is not visibly damaged (Figure 8(c)). However, before use, the grain structure of alumina seems to be merged together (Figure 8(a)), while after use, the borders between the grains became more evident and sharply defined (Figure 8(c)). This could be indicative of slight intergranular corrosion.

Finding a suitable reactor material is, however, complex because the reactor wall itself may have catalytic effect that can influence gasification efficiency and gas yields. There are limited numbers of papers that have been check whether the reactor wall material has a catalytic effect during the SCWG process. One study does show that a higher hydrogen output could be achieved in the SS reactors due to the ability of SS to catalyse the WGS reaction. Inconel-625 reactors were found to be more effective for the synthesis of methane and light hydrocarbons due to its ability to promote the CO methanation reaction [50]. Another study found that the highest hydrogen yield was obtained in the SS reactor, whilst Inconel and ceramic reactors tended to produce higher methane yields [88]. Cost considerations (Inconel-625 is much more expensive than SS) and the promotion of WGS reaction make SS more likely to be used.

A co-current reactor design with the right materials of construction might avoid corrosion during SCWG altogether but this needs to be tested. The use of catalysts (without salt content) that could reduce SCWG operation temperatures to 400 °C instead of 600 °C may reduce corrosion without compromising the gasification efficiency. Pre-treatment of biomass to remove alkaline compounds would also help to suppress reactor corrosion problem but this will bring additional cost to the feedstock used in the SCWG process. A complete corrosion control strategy for SCWG may require all the above-mentioned corrosion control measures.

5. A Potential Route to Lowering the Energy Costs of SCWG: Integration of SCWG with Biorefinery Process

Energy inefficiency is one of the barriers to the commercialisation of SCWG due to the high cost of heating the feedstock and water to supercritical conditions. The integration of SCWG with a biorefinery process such as gas fermentation is potentially a way to tackle the 'Catch 22' that has held back the development of SCWG for industrial application [70]. A recent paper demonstrated how continuous SCWG of guaiacol could be integrated with the continuous gas fermentation of CO_2 and H_2 by the cell factory, *Cupriavidus necator*, to produce (R,R)-2,3-butanediol and isopropanol via detailed simulation in Aspen HYSYS [70]. The hydrogen generated during SCWG overcomes the energy inefficiency of biological CO_2 fixation in gas fermentation (that requires high hydrogen consumption of ~8 mol H_2/mol CO_2) and the heat generated from exothermic gas

fermentation supplies the heat required in endothermic SCWG (i.e. to heat the feedstock to supercritical conditions).

The study has certain assumptions around product yields when scaling up the photo-bioreactor proportionally to the inlet flow rates and therefore, the results would need to be initially validated at pilot scale. Even though the integration of SCWG with gas fermentation is shown to be feasible (via Aspen simulation), the techno-economics require significant investment to move from theory to benchtop to pilot scale and beyond.

6. Conclusions and Future Outlook

SCWG is a promising and potentially eco-friendly technology that rapidly decomposes biomass to produce syngas (hydrogen, methane, carbon dioxide and carbon monoxide). The selection of lignocellulosic biomass as the feedstock for the SCWG process is advantageous owing to its abundant availability, low-cost nature, environmentally friendly feature and high hydrogen yields at supercritical conditions. The gasification efficiencies of many biomass types such as agricultural waste, food waste and forestry waste have been tested at laboratory-scale using batch-mode operation at supercritical conditions. Publications that describe continuous-mode pilot-scale SCWG studies is still relatively scarce. Many papers that have been published use model compounds but experimental work that has used actual biomass as a feedstock is less common. As such the mechanism for the hydrolysis and conversion of the biomass components (e.g. cellulose, hemicellulose and lignin) to gas products (mainly hydrogen) is still unclear. Many SCWG studies have shown that elevated reaction temperatures, longer residence times and low feedstock concentrations favour WGS reaction that promote hydrogen production.

Considerable effort has been devoted to developing catalysts (particularly heterogeneous catalysts) that lower reaction temperatures (from 600 to 400 °C) whilst increasing gasification efficiency. Heterogeneous catalysts including metal-based with support material, natural mineral, red mud and hydrochars have been investigated. Results have shown that a significant enhancement of hydrogen yield is possible when compared to noncatalytic experiment, although their stability and activity for continuous run requires further investigation. More recently, the direct integration of nanocatalysts (e.g. nickel) into biomass for SCWG has shown that higher hydrogen yields are possible. A preliminary economic analysis has shown that catalytic SCWG at 400 °C is more economically feasible than non-catalytic SCWG at 600 °C.

The development of novel reactors for SCWG has been relatively slow. Most studies have used autoclaves or tubular reactors even though char formation and plugging are common in both types. Fluidized bed reactors have been investigated for continuous mode SCWG in order to address the plugging problem, however its development is constrained by complexity, high energy requirements and OPEX. Whilst SCWG is a promising technology, its scale up and commercialization has been severely hampered by five main challenges: reactor corrosion, char formation, reactor plugging, high energy consumption and operating costs. These challenges must be tackled in future work with the plans outlined below before the SCWG process could be scaled up economically. The integration of SCWG with a biorefinery process (e.g. gas fermentation to produce high value chemicals) is a promising approach to counterbalance the challenge of the energetic inefficiencies seen in both processes and to explore more economically feasible routes to utilise the hydrogen generated from SCWG.

Future studies on the SCWG of biomass should focus on following areas:

(i) **Enhancement of the gasification efficiency and hydrogen yield** via the investigation of the relationship between biomass components and gasification efficiency, and the optimisation of the operating conditions (e.g. temperature, pressure, feedstock concentration and residence time).

(ii) **Minimisation of char formation in the reactor** via achieving high temperature and high pressure in short time (rapid heating), adjustment of feedstock concentration, modification of mixing strategy of biomass feedstock and water.

(iii) **Prevention of reactor corrosion** via the development of new reactor designs or by modification of successful SCWO reactor designs with the aim of minimising the interaction of corrosive species with the reactor surface.

(iv) **The development of an eco-friendly catalyst** that can reduce reaction temperatures without compromising gasification efficiency (e.g. 400 °C instead of 600 °C) and promoting hydrogen production without losing its stability and activity during continuous operation.

(v) **Making the process feasible for scaling up** through the development of method to prepare feedstock slurry with efficient pumpability (biomass is uniformly suspended into a pumpable liquid) during

continuous operation whilst solving the energy inefficiency challenge by integrating SCWG with a biorefinery process

(vi) **The development of effective heat recovery system** to recover the heat from reactor effluent and use it to heat the feedstock.

Table 1: Compilation of literature related to non-catalytic SCWG with real biomass as the feedstock

No	Types of biomass	Compositions (wt%, dry basis)			Types of reactor and its volume capacity	Studied operating conditions	Optimised operating conditions	Gas yields	Char/tar formation	References & year of publication
		Cellulose	Hemicellulose	Lignin						
1	Almond shell	52	30	21	Batch SS-316 autoclave (100 mL)	5 g biomass + 50 to 70 g of water, 60 min, 377 to 477 °C, 23 to 48 MPa	477 °C, 48 MPa	14.5, 13.2, 12.2, 11.5 and 10.3wt% H_2 of dry biomass weight for almond, cotton cocoon, hazelnut, sunflower and walnut shells respectively	-	[11] 2004
	Cotton cocoon shell	34	11	50						
	Hazelnut shell	28	31	44						
	Sunflower shell	50	36	18						
	Walnut shell	26	23	54						
2	Wood sawdust	-	-	-	Continuous SS-316L tubing reactor (140 mL)	2 or 4.1 wt% biomass + 2 wt% CMC + 10 g water, 17 to 30 MPa, 600 to 650 °C, 9 to 46 s	2 wt% biomass, 25 MPa, 650 °C, 46 s	18.7 mol H_2/kg biomass	Plugging in the reactor and a large amount of char was observed	[24] 2006
3	Tobacco stalk	49	16	11	Batch Inconel-625-lined, tumbling autoclave (1 L)	8.3 g of biomass in 140 mL of water (5 wt% of biomass in the suspension), 500 °C, heating rate 3 °C/min, 1 hour		4.5, 4.1, 4, 3.8, 2.1 and 4.1 mol H_2/kg biomass for tobacco stalk, corn stalk, cotton stalk, sunflower stalk, corncob and oreganum stalk respectively	55, 66, 104, 19, 21 and 113 g coke/kg biomass for tobacco stalk, corn stalk, cotton stalk, sunflower stalk, corncob and oreganum stalk respectively	[49] 2007
	Corn stalk	27	27	3						
	Cotton stalk	47	13	11						
	Sunflower stalk	43	7	10						
	Corncob	32	32	3						
	Oreganum stalk	34	11	9						
4	Maize silage, Corn silage / ethanol	-	-	-	Continuous down-flow tubular reactor (Verena pilot plant)	20 kg/h feed at 360 °C, 80 kg/h water at 620 °C, 20% dry biomass, 600 °C, 28 MPa, 1.8 min, 11 wt% ethanol, 10 hours operation time		9 mol H_2/kg dry biomass	No char formation, the settled salts were separated from the reaction system by the brine removal system	[83] 2007
5	Corn cob + carboxymethyl cellulose (CMC)	-	-	-	Continuous SS-316 fluidized bed reactor	550 to 650 °C, 25 MPa, 5 to 18 wt% feedstock concentration, 2 to 3 wt% CMC concentration, 0 to 18 wt% H_2O_2 oxidant concentration, 1:5 ratio of feedstock to water flow rate, 127 g/min flow rate of preheated water	650 °C, 5 wt% feedstock concentration, 0 wt% H_2O_2 concentration	12 mol H_2/kg biomass	No reactor plugging after 5 hours running at 18 wt% feedstock concentration	[25] 2008

6	Corn cob + carboxymethyl cellulose	-	-	-	Batch Hastelloy C276 tubular reactor	550 to 650 °C, 22.5 to 27.5 MPa, 20 to 40 s, 1 to 2 wt% CMC + 2 to 4 wt% corncob feedstock	650 °C, 25 MPa, 40 s, 1 wt% CMC + 2 wt% corncob	15.2 mol H_2/kg biomass	-	[30] 2011
7	Beech sawdust	-	-	-	Batch SS and Inconel-625 reactors (5 mL)	350 (subcritical) and 400 °C (supercritical), 60 to 300 min, 30 MPa, 1.8 g biomass/5 mL water at 400 °C, 3.2 g biomass/5 mL water at 350 °C	400 °C, 120 min	0.85 and 1.3 mol H_2/kg biomass for Inconel and SS reactors respectively	0.3 mg solid char/g biomass for Inconel and SS reactors	[50] 2013
8	Empty fruit bunches from oil palm	-	-	-	Batch SS tubing reactor (13 mL)	380 °C, 24 MPa, 0.05 to 0.5 g biomass + 8 mL water feedstock, heating rate 10 °C/min, 8 to 32 min	0.3 g biomass, 32 min	74 mol H_2/L of feedstock	Char was observed after each experiment	[31] 2015
9	Almond shell	31	31	36	Batch SS microreactor (23 mL)	440 °C, 25 MPa, 1 wt% feed mixture (0.05 g biomass + 5 g water), 15 min		13, 12.5, 17, 20.5, 17.5 and 13.5% HGE for rice straw, canola straw, almond shell, barley straw, wheat straw and walnut shell respectively	-	[37] 2016
	walnut shell	27	27	40						
	barley straw	32	29	30						
	canola stalk	38	29	20						
	rice straw	38	25	28						
	wheat straw	39	26	27						
10	Wheat straw	40	27	19	Batch SS-316 micro tubular reactor (26 mL)	1 wt% mixture (0.06 g biomass + 6 g water), 440 °C, 25 MPa, 0 to 30 min	10 min for wheat straw, 15 min for almond shell, 20 min for walnut shell	7.3, 4.1 and 4.6 mol H_2/kg wheat straw, almond shell and walnut shell respectively	Char was observed after each experiment	[32] 2016
	walnut shell	36	25	38						
	almond shell	31	33	35						
11	Beech sawdust, malt spent grains	-	-	-	Batch Inconel-625, SS and ceramic (Al_2O_3) autoclave reactor (24 mL)	400 °C, 30 MPa, 15wt% feedstock, 16 hours		Beech sawdust: 0.6, 1.2 and 0.7 mol H_2/kg biomass for Inconel-625, SS and ceramic reactor respectively Malt spent grains: 0.45, 0.4 and 0.3 mol H_2/kg biomass for Inconel-625, SS and ceramic reactor respectively	Coke formation was observed after the experiment	[88] 2017

Table 2: Compilation of literature related to catalytic SCWG with homogeneous catalysts by using real biomass as the feedstock

No	Types of biomass	Compositions (wt%, dry basis)			Types of reactor and its volume capacity	Studied operating conditions	Optimised operating conditions	Gas yields	Char/tar formation	References & year of publication
		Cellulose	Hemicellulose	Lignin						
1	Clover grass	-	-	-	Continuous nickel alloy Inconel-625 flow reactor	625 to 700 °C, 25 MPa, 5 wt% feed, 3 g/min feed flow rate, 100 ppm $KHCO_3$ catalyst	700 °C	0.27 to 0.4 gasification yield (kg C gas / kg biomass)	-	[85] 2006
2	Sunflower stalk	43	7	10	Batch Inconel-625, tumbling autoclave (1 L)	8.3 g of biomass, 0.8 g of catalyst (K_2CO_3), 140 ml of water, 500 °C, heating rate of 3 °C/min, 31 MPa, 1 hour		3.7 and 9.7 mol H_2/kg biomass for noncatalyst and K_2CO_3 respectively	19 and 90 g coke/kg biomass for noncatalyst, K_2CO_3 respectively	[47] 2008
	Corncob	32	32	3				2.1 and 8 mol H_2/kg biomass for noncatalyst and K_2CO_3 respectively	22 and 22 g coke/kg biomass for noncatalyst and K_2CO_3 respectively	
3	Cauliflower residue	31	5	4	Continuous Inconel-625 down-flow tubular reactor	600 °C, 35 MPa, 8 wt% biomass + 0.5 wt% xanthan, 0.8 wt% catalyst (K_2CO_3/Trona), 0.3 min		K_2CO_3: 12.9, 17, 9.9, 9.7, 11.7 mol H_2/kg biomass for cauliflower residue, tomato residue, hazelnut shell, acorn, extracted acorn respectively Trona: 12.5, 10.4, 11, 26.7, 11.2 mol H_2/kg biomass for cauliflower residue, tomato residue, hazelnut shell, acorn, extracted acorn respectively	Char was observed after each experiment (2 hours duration)	[40] 2011
	acorn	25	17	13						
	Tomatoes residue	24	17	22						
	Extracted acorn	39	15	24						
	hazelnut shell	38	12	40						
4	Peanut shell	-	-	-	Batch SS-316 autoclave (140 mL)	400 °C, 23 MPa, 20 mins, heating rate 17 °C/min, 1 g catalyst (LiOH / Na_2CO_3 / NaOH / K_2CO_3 / KOH / $Ca(OH)_2$ / $ZnCl_2$), 1 g biomass + 0.3 g CMC	KOH > $Ca(OH)_2$ > K_2CO_3 > LiOH > ZnCl2 > NaOH > Na_2CO_3	2.9, 7, 6.7, 5.6, 5.3, 5.2, 3.5 and 3.1 mol H_2/kg biomass for no catalyst, KOH, $Ca(OH)_2$, K_2CO_3, LiOH, $ZnCl_2$, NaOH and Na_2CO_3 respectively	K_2CO_3 - no tar formation, ZnCl2, NaOH- there was tar and char formation, No information for other catalysts	[53] 2014

5	Canola meal, wheat straw, timothy grass	-	-	-	Batch SS-316 tubular reactor	450 to 650 °C, 25 to 100% catalyst (K_2CO_3) loading, 26 MPa, 5 mass ratio of water to biomass, 0.65 g biomass, heating rate 30 °C/min, 50 min	650 °C and 100% catalyst loading for canola meal and wheat straw, 550 °C and 100% catalyst loading for timothy grass	3.4, 2.1 and 1.8 mol H_2/kg biomass for canola meal, wheat straw and timothy grass respectively	-	[52] 2016
6	Aloe vera rind	58	16	14	Batch SS-316 fixed bed tubular reactor	400 to 600 °C, 1:5 biomass to water ratio (1.8 g biomass + 9 mL water) to 1:10 (0.9 g biomass + 9 mL water), 15 to 45 min, 24 MPa, 1 to 2 wt% catalyst (NaOH / K_2CO_3)	600 °C, 1:10 biomass to water ratio, 45 min, 2 wt% K_2CO_3	3.6, 3.3, 4.8, 3.5, 3.5, 3.7 and 4.5 mol H_2/kg biomass for aloe vera rind, banana peel, coconut shell, lemon peel, pineapple peel, orange peel and bagasse respectively	Char was observed after each experiment	[12] 2016
	banana peel	65	8	10						
	coconut shell	14	32	46						
	lemon peel	13	5	2						
	orange peel	14	6	2						
	pineapple peel	-	16	-						
	sugarcane bagasse	48	24	32						
7	Pinecone	37	38	25	Batch SS-316 tubular reactor	300 to 550 °C, 22 MPa, 10 to 25 wt% feed concentration, 15 to 60 min, 30 wt% catalysts (Na_2CO_3 / NaOH / KOH)	550 °C, 10 wt% feed concentration, 60 min	3.3, 2.7 and 2 mol H_2/kg biomass for KOH, NaOH and Na_2CO_3 respectively	hydrochar and tar were observed after each experiment	[18] 2017
8	Waste cooking oil	-	-	-	Batch SS-316 tubular fixed bed reactor	375 to 675 °C, 25 to 40 wt% feed concentration, 15 to 60 min, 5 wt% catalyst (Na_2CO_3 / K_2CO_3), 24 MPa	675 °C, 25 wt% feed concentration, 60 min, K_2CO_3 > Na_2CO_3	5.2, 7.6 and 8.5 mol H_2/kg biomass for no catalyst, Na_2CO_3 and K_2CO_3 respectively	-	[13] 2019
9	White poplar (Populus alba L.) sawdust	56	15	20	SS316 batch autoclave (100 mL)	400 to 600 °C, 24 to 45 MPa, 60 min, 1.2 g of biomass + 15 mL water, 0.12 g K_2CO_3 as the catalyst, heating rate of 10 to 15 °C/min	600 °C, 45 MPa	12.6 and 16.4 mol H_2/kg biomass for no catalyst and K_2CO_3 respectively	11.4 C% of tar and char	[82] 2020
	Isolated hemicellulose from the white poplar	3.5	92.5	4				13.5 and 20.3 mol H_2/kg biomass for no catalyst and K_2CO_3 respectively	6.9 C% of tar and char	
10	Soybean straw	-	-	-	Batch SS-316 fixed bed tubular reactor	300 to 500 °C, 1:5 and 1:10 biomass-to-water ratio, 0.13 and 0.8 mm biomass particle size, 30 to 60 min, 22 to 25 MPa, 3 wt% KOH catalyst solution, heating rate of 30 °C/min	500 °C, 1:10 biomass-to-water ratio, 0.13 mm particle size, 45 min	6.6 and 7.6 mol H_2/kg biomass for noncatalyst and KOH respectively	6.3 to 8.1 wt% char was formed	[23] 2020
	Flax straw	-	-	-				3.8 and 6 mol H_2/kg biomass for noncatalyst and KOH respectively	-	

Table 3: Compilation of literature related to catalytic SCWG with heterogeneous catalysts by using real biomass as the feedstock

No	Types of biomass	Compositions (wt%, dry basis)			Types of reactor and its volume capacity	Studied operating conditions	Optimised operating conditions	Gas yields	Char/tar formation	References & year of publication
		Cellulose	Hemicellulose	Lignin						
1	Sunflower stalk	43	7	10	Inconel-625-lined, tumbling batch autoclave (volume of 1 L)	8.3 g of biomass (5.5 wt% biomass), 0.8 g of catalyst (0.5 wt% catalysts: Trona, red mud and Raney Ni), 140 ml of water, 500 °C, heating rate of 3 °C/min, 31 MPa, 1 hour	Trona > red mud > Raney Ni	3.7, 9.4, 8.1 and 8 mol H_2/kg biomass for no catalyst, Trona, red mud and Raney Ni respectively	19, 160, 358 and 31 g coke/kg biomass for noncatalyst, Trona, red mud and Raney Ni respectively	[47] 2008
	Corncob	32	32	3				2.1, 12, 5.7 and 3.5 mol H_2/kg biomass for no catalyst, Trona, red mud and Raney Ni respectively	22, 41, 29 and 17 g coke/kg biomass for noncatalyst, Trona, red mud and Raney Ni respectively	
2	Liquefied switchgrass biocrude	-	-	-	Continuous Inconel-600 packed bed tubular reactor	600 °C, 25 MPa, 0.6 mL/min biocrude flow rate, catalysts (Ru/TiO_2, Ru/ZrO_2, Ni/TiO_2, Ni/ZrO_2, Co/TiO_2, Co/ZrO_2), 2 hours continuous run, $Ru/MgAl_2O_4$, $Ni/MgAl_2O_4$ and $Co/MgAl_2O_4$ charred immediately and no results could be obtained.	Ni/ZrO_2 > Ru/TiO_2 > Co/ZrO_2 > Ni/TiO_2 > Co/TiO_2 > Ru/ZrO_2	0.8, 0, 0.65, 1, 0.6 and 0.7 mol H_2/mol C reacted for Ru/TiO_2, Ru/ZrO_2, Ni/TiO_2, Ni/ZrO_2, Co/TiO_2, Co/ZrO_2 respectively	Charring of all the catalysts was seen at the reactor entrance	[58] 2011
3	Sugarcane bagasse	35	36	16	Batch SS-316 reactor (6 mL)	400 °C, 0.4 g Ru/TiO_2 or 0.2 g Ru/AC, 0.1 g biomass, 0 to 3 g water, 5 to 30 mins	3 g water, 15 min	0.6, 2.3 and 3.2 mol H_2/kg biomass for no catalyst, Ru/AC and Ru/TiO_2 respectively	Char was observed after each experiment	[33] 2012
4	Cotton stalk	51	12	19	Batch SS autoclave reactor (100 mL)	300 to 600 °C, 10 wt% of mineral catalysts (Trona, Dolomite and Borax), 1.2 g of biomass/15 mL of water, heating rate 6 K/min, 1 hour	600 °C, Trona > Borax > Dolomite	Non-catalyst: 9.3 and 8 mol H_2/kg biomass for tobacco and cotton stalks respectively Trona: 11.4 and 10.6 mol H_2/kg biomass for tobacco and cotton stalks respectively	Char was observed after each experiment	[2] 2012
	tobacco stalk	50	16	13						

5	Birchwood bark	-	-	-	Batch SS reactor (50 mL)	380 °C, 23 MPa, 2 wt% feed concentration (0.2 g feedstock + 9.8 g water), 120 mg metal loading of Ni and 6 mg metal loading of Ru (Ni/α-Al_2O_3, Ni/hydrotalcite, Raney nickel, Ru/AC and Ru/γ-Al_2O_3) into the reactor, 5 to 60 min	15 min for noncatalytic condition, 60 min for catalytic condition	15 min: 1.3, 30, 23, 35, 9 and 13 mol H_2/kg feed for no catalyst, Raney Ni, Ni/α-Al_2O_3, Ni/hydrotalcite, Ru/AC and Ru/γ-Al_2O_3 60 min: 45, 46, 63, 20 and 23 mol H_2/kg feed for Raney Ni, Ni/α-Al_2O_3, Ni/hydrotalcite, Ru/AC and Ru/γ-Al_2O_3	-	[57] 2012
6	Sawdust	-	-	-	Batch Inconel reactor (75 mL)	1 g Ru/Al_2O_3 + 1.2 g CaO, 1 g of biomass in 20 mL water, 550 °C, 10 min, 36 MPa		52 mol% H_2, 39 mol% CH_4, 5 mol% CO, 1 mol% CO_2, 3 mol% C_2-C_4 gases	No significant tar formation was observed	[66] 2013
7	Peanut shell	-	-	-	Batch SS-316 autoclave (140 mL)	400 °C, 23 MPa, 20 min, heating rate 17 °C/min, 1 g catalyst (Raney Ni, dolomite and olivine), 1 g biomass + 0.3 g CMC	Raney Ni > olivine > dolomite	2.9, 10.8, 4.2 and 3.9 mol H_2/kg biomass for no catalyst, Raney Ni, olivine and dolomite respectively	Raney Ni - no tar formation No information for other catalysts	[53] 2014
8	Pinewood	39	34	12	Batch SS-316 reactor (6 mL)	550 °C, 7:1 water to biomass weight ratio (4.6 g H_2O was fixed), 30 mins, 0.65 g of Ni/CeO_2/Al_2O_3 or calcined dolomite or 0.4 g of 1.7 M KOH, heating rate 30 °C/min	KOH > Ni/CeO_2/Al_2O_3 > dolomite	0.8, 1.3, 1 and 5.6 mol H_2/kg biomass for no catalyst, Ni/CeO_2/Al_2O_3, Dolomite and KOH respectively	0.1 to 0.4 g of char was formed at the optimised conditions	[26] 2014
9	Hazelnut shell	38	40	12	Batch SS reactor (100 mL)	300 to 600 °C, 9 to 41 MPa, 1.2 g of biomass in 15 mL water, 0.12 g catalyst (Trona / Dolomite / Borax), heating rate 6 K/min, 1 hour	600 °C, 37 MPa, Trona catalyst	9.8, 10.8 and 10.8 mol H_2/kg biomass for hazelnut shell, walnut shell and almond shell respectively	Tar and char were observed after each experiment	[39] 2014
	walnut shell	42	35	16						
	almond shell	43	29	23						
10	Sugarcane bagasse	-	-	-	Batch SS-316 reactor (25 mL)	400 °C, 24 MPa, 15 min, 0.08 g biomass loading, 6.5 g water loading, Cu promoted Ni/γ-Al_2O_3 nanocatalyst with 2.5 to 30 wt% Ni and 0.6 to 7.5 wt% Cu loadings	20 wt% Ni and 5 wt% Cu loadings for the preparation of Cu promoted Ni/Y-Al_2O_3	3.3 and 11.8 mol H_2/kg biomass for no catalyst and Cu promoted Ni/γ-Al_2O_3 respectively	-	[56] 2015

11	Sugarcane bagasse	-	-	-	Batch SS-316 reactor (25 mL)	400 °C, 24 MPa, 5 to 30 mins, 0.05 to 0.25 g biomass loading, 6.5 g water loading, nanocatalysts Ni/CNT or Ni-Cu/CNT (5 to 20 wt% Ni, 0 to 7.5 wt% Cu)	0.05 g biomass loading, 20 min, 20 wt% Ni and 5 wt% Cu on Ni-Cu/CNT	3, 22 and 23 mol H_2/kg biomass for no catalyst, Ni/CNT and Ni-Cu/CNT respectively	-	[36] 2015
12	Pinewood, Wheat straw	-	-	-	Batch SS-316 tubular reactor	300 to 500 °C, 1:5 (1.8 g biomass + 9 mL water) to 1:10 (0.9 g biomass + 9 mL water) Ni-impregnated biomass to water ratio, 15 to 45 min, 24 MPa	500 °C, 1:10 biomass to water ratio, 45 min	No catalyst: 1.1 and 3.5 mol H_2/kg biomass for pinewood and wheat straw respectively Catalyst: 2.8 and 5.6 mol H_2/kg biomass for pinewood and wheat straw respectively	2 to 8.2 wt% biochar was formed after each experiment. SbCWG (300 °C) led to relatively higher biochar yield, which gradually decreased in SCWG (400 and 500 °C)	[19] 2016
13	Fruit pulp from fruit juice factory	31	37	17	Batch Inconel-625 reactor (200 mL)	400 to 600 °C, 0 to 60 min, 2.5 to 10 wt% biomass to water ratio, 0 to 40 wt% catalyst (5 wt% Ru on activated carbon, 811 m^2/g surface area) to biomass ratio	2.5 wt% biomass to water ratio, 600 °C, 30 min, 30 wt% Ru/AC to biomass ratio	15.8 and 55 mol H_2/kg biomass for no catalyst and Ru/AC respectively	Char was observed after each experiment	[15] 2016
14	Canola meal,	-	-	12	Batch SS-316 tubular reactor	450 to 650 °C, 25 to 100% catalyst (20Ni-0.36Ce/Al_2O_3) loading, 26 MPa, 5 mass ratio of water to biomass, 0.65 g biomass, heating rate 30 °C/min, 50 min	650 °C and 50% catalyst loading for canola meal and timothy grass, 550 °C and 100% catalyst loading for wheat straw	1.9, 2 and 1.5 mol H_2/kg biomass for canola meal, wheat straw and timothy grass respectively	Char was observed after each experiment	[52] 2016
	wheat straw,	-	-	16						
	timothy grass	-	-	18						
15	Wheat straw	-	-	-	Batch SS-316 tubular reactor	300 to 550 °C, 20 (2 g biomass + 8 mL water) to 35 wt% feed concentration, 40 to 70 min, 5 wt% Ru/Al_2O_3 or Ni/Si- Al_2O_3, 22 MPa	550 °C, 20 wt% feed concentration, 60 min	3, 4.2 and 5.1 mol H_2/kg biomass for no catalyst, Ru/Al_2O_3 and Ni/Si-Al_2O_3 respectively	7.2 wt% biochar was formed under optimised conditions	[21] 2018
16	Almond shell	41	20	33	Batch SS-316 tubular microreactor (26 mL)	400 to 460 °C, 5 to 30 min, 0.01 to 0.03 feedstock/water ratio, 27 MPa, catalysts (hydrochars after SCWG of wheat straw and C. glomerata	460 °C, 10 min, 0.01 feed/water ratio	7.9, 10.8 and 11.6 mol H_2/kg biomass for no catalyst, WS hydrochar and macroalgae	Char was observed after each experiment	[16] 2018

						macroalgae), 0.4 weight ratio of catalyst to biomass		hydrochar respectively		
17	Waste cooking oil	-	-	-	Batch SS-316 tubular fixed bed reactor	375 to 675 °C, 25 to 40 wt% feed concentration, 15 to 60 min, 5 wt% catalyst (Ru/Al_2O_3 or $Ni/Si\text{-}Al_2O_3$), 24 MPa	675 °C, 25 wt% feed concentration, 60 min, Ru/Al_2O_3 > $Ni/Si\text{-}Al_2O_3$	5.2, 10.2 and 9.5 mol H_2/kg biomass for no catalyst, Ru/Al_2O_3 and $Ni/Si\text{-}Al_2O_3$ respectively	-	[13] 2019
18	Sugarcane bagasse	40	31	20	Batch SS-316 tubular hydrothermal reactor (20 mL)	300 to 500 °C, 1:8 to 1:2 nano-nickel impregnated biomass to water ratio (by weight), 22 to 25 MPa, 50 min	500 °C, 1:8 biomass to water ratio, bagasse > mosambi peel	13.8 and 9.5 mol H_2/kg biomass for bagasse and mosambi peel respectively	Char was observed after each experiment	[20] 2019
	mosambi peels	35	27	23						
19	Empty palm fruit bunches (EFBs)	-	-	-	Batch SS tubular reactor (13 mL)	0.3 g of EFBs + 5 wt% of the catalyst in 8 mL of water, 380 °C, 8 to 32 min, 5 to 15 wt% Ni and 5 to 15 wt% Zn on CaO, heating rate 10 °C/min	5 wt% ZnO with 5 wt% Ni on CaO (5ZnO/5Ni–CaO), 32 min	135 mmol H_2/mL of gas	Tarry compounds were observed after each reaction	[55] 2019
20	Wheat straw	-	-	-	Batch SS-316L autoclave (140 mL)	450 °C, 25 MPa, 0.5 g wheat straw + 0.3 g CMC + 10 g water, 0.2 g catalyst (Ni/MgO, Fe/MgO, Cu/MgO, Ni/ZnO, Ni/Al_2O_3, Ni/ZrO_2), heating rate 9 K/min, 20 min	Ni/MgO > Fe/MgO > Cu/MgO > Ni/ZnO > Ni/Al_2O_3 > Ni/ZrO_2	3.8, 11.6, 9.2, 8.1, 10.3, 10 and 10.8 mol H_2/kg biomass for no catalyst, Ni/MgO, Fe/MgO, Cu/MgO, Ni/Al_2O_3, Ni/ZrO_2 and Ni/ZnO	-	[48] 2019
21	Banana pseudo-stem	-	-	-	Batch Inconel tubular reactor (25 mL)	Nickel (1 mol/kg biomass), Ruthenium (0.8 mol/kg biomass) and iron (0.8 mol/kg biomass) are separately impregnated into biomass, 300 to 600 °C, 1:10 biomass-to-water weight ratio, 60 min, 22 to 25 MPa	600 °C, nickel (5.4 wt%) > ruthenium (7.1 wt%) > iron (4.4 wt%) impregnated biomass	4.2 mol H_2/kg biomass for raw biomass; 11.1, 8.8 and 8 mol H_2/kg biomass for nickel, ruthenium and iron impregnated biomass respectively	Char was formed after each experiment	[22] 2020
22	Food waste	-	-	-	Batch Hastelloy reactor (200 mL)	Lanthanum (La) promoted Ni/Al_2O_3 catalysts with different La loading content (3 to 15 wt%), 420 to 480 °C, 26 to 30 MPa, 6 g food waste + 66 mL water + 0.7 g catalyst (1 wt% catalyst loading), 40 min, 80 rpm stirring	480 °C, 9 wt% La loading on Ni/Al_2O_3	2.6 and 8 mol H_2/kg biomass for noncatalyst and 9 wt% La loading on Ni/Al_2O_3 respectively	-	[17] 2020

Table 4: Physical characteristics of the micro-sized and nano-sized heterogeneous catalysts investigated for the SCWG of real biomass

Biomass	Catalyst	Catalyst size (μm/nm)	BET surface area (m^2/g)	Total pore volume (mL/g)	Metal loading (wt %)	Metal dispersion (%)	Hydrogen yield	Reference, year of publication
Liquefied switchgrass biocrude	Ru/TiO_2	8.4 nm	37	0.2	1.5 (Ru)	-	0.8 mol H_2/mol C reacted	[58] 2011
	Ru/ZrO_2	9.8 nm	51	0.3	1.5 (Ru)	-	0 mol H_2/mol C reacted	
	Ni/TiO_2	8.3 nm	32	0.1	10 (Ni)	-	0.7 mol H_2/mol C reacted	
	Ni/ZrO_2	9.6 nm	43	0.2	10 (Ni)	-	1 mol H_2/mol C reacted	
	Co/TiO_2	7.7 nm	32	0.1	10 (Co)	-	0.6 mol H_2/mol C reacted	
	Co/ZrO_2	9.3 nm	42	0.2	10 (Co)	-	0.7 mol H_2/mol C reacted	
Sugarcane bagasse	Ru/TiO_2	-	24	-	2 (Ru)	27 (Ru)	3.2 mol H_2/kg biomass	[33] 2012
	Ru/C	-	768	-	5 (Ru)	51 (Ru)	2.3 mol H_2/kg biomass	
Birchwood bark	Raney Ni	35 μm	78	-	93 (Ni)	13.4 (Ni)	45 mol H_2/kg feed (birchwood bark + water)	[57] 2012
	$Ni/\alpha\text{-}Al_2O_3$	118 μm	8	-	5 (Ni)	4.5 (Ni)	46 mol H_2/kg feed	
	Ni/Hydrotalcite	1 μm	12	-	5 (Ni)	1.3 (Ni)	63 mol H_2/kg feed	
	Ru/AC	18 μm	900	-	5 (Ru)	41 (Ru)	20 mol H_2/kg feed	
	$Ru/Y\text{-}Al_2O_3$	40 μm	90	-	5 (Ru)	16.7 (Ru)	23 mol H_2/kg feed	
Pinewood	$Ni/CeO2/Al_2O_3$	-	154	0.44	7.2 (Ni)	1 (Ni)	1.3 mol H_2/kg biomass	[26] 2014
Sugarcane bagasse	Cu promoted $Ni/\gamma\text{-}Al_2O_3$	8.5 nm	173	0.6	20 (Ni)	-	11.8 mol H_2/kg biomass	[56] 2015
Sugarcane bagasse	Ni/CNT	14.3 nm	178	0.4	20 (Ni)	-	22 mol H_2/kg biomass	[36] 2015
	Ni-Cu/CNT	15.4 nm	169	0.4	20 (Ni)	-	23 mol H_2/kg biomass	
Cellulose, lignin, canola meal, wheat straw, timothy grass	Al_2O_3	11 nm	262	0.7	-	-	0.4 mol H_2/kg cellulose, 1.5 mol H_2/kg lignin	[52] 2016
	$Ni\text{-}0.36Ce/Al_2O_3$	10 nm	202	0.5	20 (Ni)	2.1 (Ni)	1.9 mol H_2/kg cellulose, 2.2 mol H_2/kg lignin, 1.9 mol H_2/kg canola meal, 2 mol H_2/kg wheat straw, 1.5 mol H_2/kg timothy grass	
	Ni/Al_2O_3	10 nm	195	0.5	20 (Ni)	1.7 (Ni)	1.2 mol H_2/kg cellulose, 0.8 mol H_2/kg lignin	
	Ru/Al_2O_3	12 nm	226	0.7	5 (Ru)	8.7 (Ru)	0.9 mol H_2/kg cellulose, 1.1 mol H_2/kg lignin	
Almond shell	Wheat straw hydrochar	-	149	0.1	-	-	10.8 mol H_2/kg biomass	[16] 2018
	C. glomerata macroalgae hydrochar	-	58	0.04	-	-	11.6 mol H_2/kg biomass	
Empty palm fruit bunches	5ZnO/5Ni–CaO	50.4 nm	3	0.01	5 (Ni)	-	135 mmol H_2/mL of gas	[55] 2019
Food waste	Ni/Al_2O_3	12.6 nm	123.6	0.4	15 (Ni)	-	4.1 mol H_2/kg biomass	[17] 2020
	3wt% La loading on Ni/Al_2O_3	12.9 nm	113.6	0.4			4.5 mol H_2/kg biomass	
	6wt% La loading on Ni/Al_2O_3	14.1 nm	111.7	0.4			4.8 mol H_2/kg biomass	
	9wt% La loading on Ni/Al_2O_3	13.2 nm	103.9	0.3			5.6 mol H_2/kg biomass	
	12wt% La loading on Ni/Al_2O_3	13.3 nm	104.5	0.4			4.8 mol H_2/kg biomass	

	15wt% La loading on Ni/Al_2O_3	12.9 nm	94.5	0.3			4.5 mol H_2/kg biomass	

Table 5: Proximate and ultimate analysis data of wheat straw [21]

Proximate analysis (wt%, dry)		**Ultimate analysis (wt%, dry)**	
Moisture content (wt%)	7.4	C	44.1
Ash content	4.4	H	6
Volatile matter	56.7	O	45.1
Fixed carbon	31.5	N	0.4
		S	0.01

Table 6: Mass balance for modelling of catalytic SCWG with wheat straw biomass at 400 °C operating temperature (HP = high pressure)

Parameters		**Water**	**HP water**	**Heated water**	**SCW**	**Biomass**	**HP biomass**	**Products**	**Products 2**	**Products 3**	**Liquid products**	**Gas products**	**Methane**	**Air**	**Flue gas**	**Chimney**
T (°C)		25	26.8	350	400	25	26.3	400	234.5	96.8	90	90	20	20	1700	50
P (kPa)		101	2.21 x 10^4	2.21 x 10^4	2.21 x 10^4	101	2.21 x 10^4	2.21 x 10^4	2.21 x 10^4	101	101	101	200	200	200	200
Mass flow (kg/h)		1.8 x 10^4	1.8 x 10^4	1.8 x 10^4	1.8 x 10^4	2100	2100	2.01 x 10^4	2.01 x 10^4	2.01 x 10^4	1.58 x 10^4	4223.78	348.1	6491.3	6839.5	6839.5
Partial mass flow (kg/h)	**Biomass**	-	-	-	-	1000	1000	-	-	-	-	-	-	-	-	-
	Water	1.8 x 10^4	1.8 x 10^4	1.8 x 10^4	1.8 x 10^4	1000	1000	18482.2	18482.2	18482.2	15734.8	2747.4	-	-	781.9	781.9
	Hydrogen	-	-	-	-	-	-	90.77	90.77	90.77	-	90.77	-	-	-	-
	Carbon dioxide	-	-	-	-	-	-	1233.8	1233.8	1233.8	0.15	1233.6	-	-	955	955
	Methane	-	-	-	-	-	-	117.5	117.5	117.5	-	117.5	348.1	-	-	-
	Carbon monoxide	-	-	-	-	-	-	15.6	15.6	15.6	-	15.6	-	-	-	-
	Ash	-	-	-	-	-	-	39.3	39.3	39.3	39.3	-	-	-	-	-
	Oxygen	-	-	-	-	-	-	-	-	-	-	-	-	1511.9	123.2	123.2
	Nitrogen	-	-	-	-	-	-	-	-	-	-	-	-	4979.4	4979.4	4979.4
	$Mg(NO_3)_2.6H_2O$	-	-	-	-	84.3	84.3	84.3	84.3	84.3	84.3	-	-	-	-	-
	$Ni(NO_3)_2.6H_2O$	-	-	-	-	15.7	15.7	15.7	15.7	15.7	15.7	-	-	-	-	-

Table 7: Mass balance for modelling of non-catalytic SCWG with wheat straw biomass at 600 °C operating temperature (HP = high pressure)

Parameters		**Water**	**HP water**	**Heated water**	**SCW**	**Biomass**	**HP biomass**	**Products**	**Products 2**	**Products 3**	**Liquid products**	**Gas products**	**Methane**	**Air**	**Flue gas**	**Chimney**
T (°C)		25	26.8	350	600	25	26.3	600	329.5	98.3	90	90	20	20	1700	50
P (kPa)		101	2.21 x 10^4	2.21 x 10^4	2.21 x 10^4	101	2.21 x 10^4	2.21 x 10^4	2.21 x 10^4	101	101	101	200	200	200	200
Mass flow (kg/h)		1.8 x 10^4	1.8 x 10^4	1.8 x 10^4	1.8 x 10^4	2000	2000	2 x 10^4	2 x 10^4	2 x 10^4	1.58 x 10^4	4223.78	561.5	1.01 x 10^4	1.07 x 10^4	1.07 x 10^4
	Biomass	-	-	-	-	1000	1000	-	-	-	-	-	-	-	-	-

Partial mass flow (kg/h)	**Water**	1.8 x 10^4	1.8 x 10^4	1.8 x 10^4	1.8 x 10^4	1000	1000	18482.2	18482.2	18482.2	15734.8	2747.4	-	-	1261.1	1261.1
	Hydrogen	-	-	-	-	-	-	90.77	90.77	90.77	-	90.77	-	-	-	-
	Carbon dioxide	-	-	-	-	-	-	1233.8	1233.8	1233.8	0.15	1233.6	-	-	1540.3	1540.3
	Methane	-	-	-	-	-	-	117.5	117.5	117.5	-	117.5	561.5	-	-	-
	Carbon monoxide	-	-	-	-	-	-	15.6	15.6	15.6	-	15.6	-	-	-	-
	Ash	-	-	-	-	-	-	39.3	39.3	39.3	39.3	-	-	-	-	-
	Oxygen	-	-	-	-	-	-	-	-	-	-	-	-	2351.9	112	112
	Nitrogen	-	-	-	-	-	-	-	-	-	-	-	-	7745.7	7745.7	7745.7

Table 8: Values for different parameters in the modelling of SCWG with guaiacol as the feedstock

Parameters	**Values**
Operating plant life	20 years
Operating hours	8760 hours
Length of plant start-up	20 weeks
Water cost	£ 1.21/m^3
Electricity cost	£ 0.124/kWh
Natural gas (methane) cost	£ 0.028/kWh
Cost for wheat straw [89]	£ 93/tonne
Cost for nickel nitrate hexahydrate	£ 0.77/kg
Cost for magnesium nitrate hexahydrate	£ 0.15/kg

Table 9: Economic analysis results for catalytic SCWG at 400 °C and non-catalytic SCWG at 600 °C

Parameters	**400 °C (catalytic)**	**600 °C (non-catalytic)**
Total capital cost (USD)	6,037,450	7,823,040
Total operating cost (USD/year)	7,817,240	9,500,360
Total raw material cost (including biomass, water, methane and catalyst) (USD/year)	4,295,390	5,384,810
Total utilities cost (USD/year)	466,542	888,246
Electricity (kW)	300.74	302.23

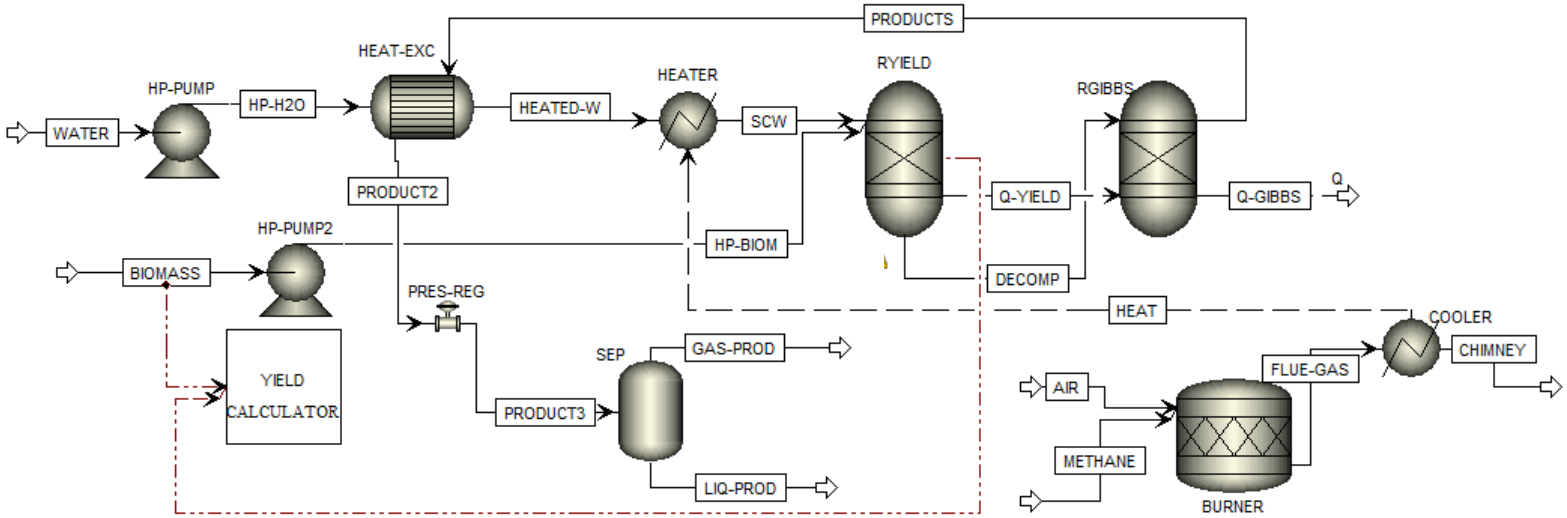

Figure 1: Flow diagram of the SCWG process with wheat straw as the feedstock

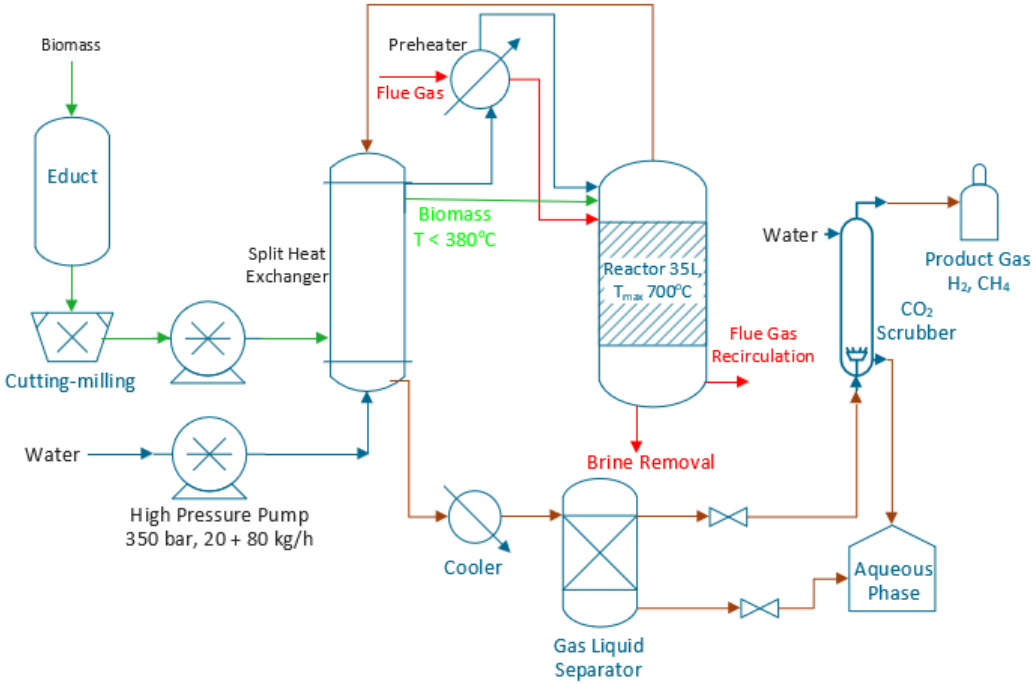

Figure 2: Process flow diagram of VERENA pilot plant, redrawn with reference to [83]

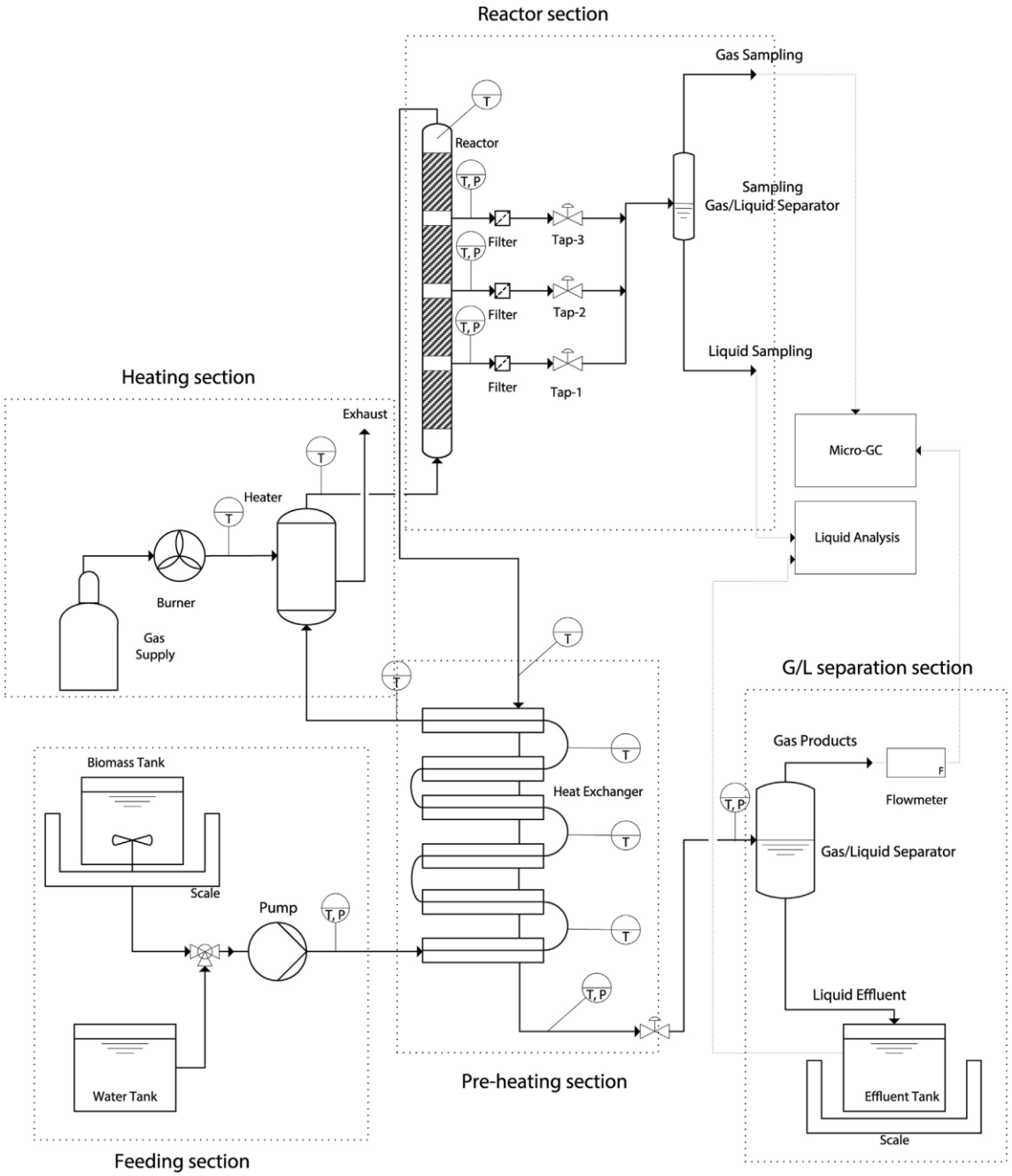

Figure 3: Process flow diagram of TU Delft/Gensos semi-pilot scale, adapted with permission from [84]

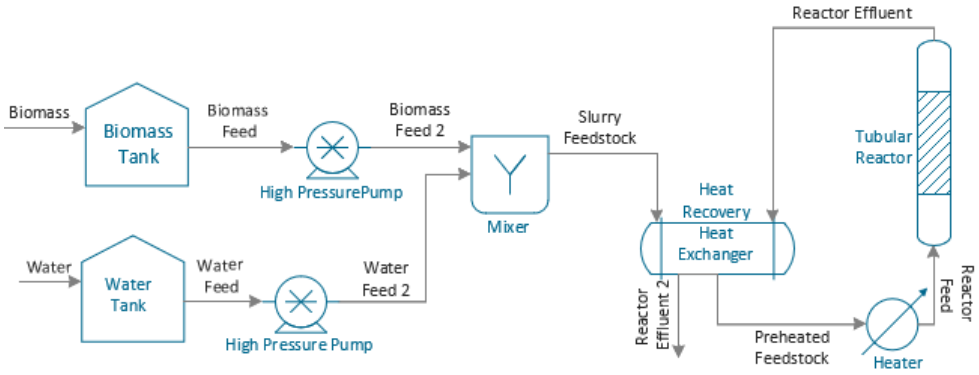

Figure 4: Mixing water and biomass at room temperature before heating the slurry to supercritical conditions, drawn with reference to [84]

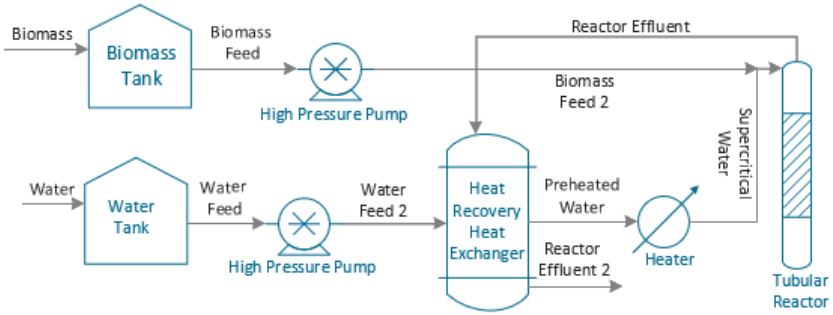

Figure 5: Injecting a biomass feedstock slurry at room temperature into SCW, drawn with reference to [25]

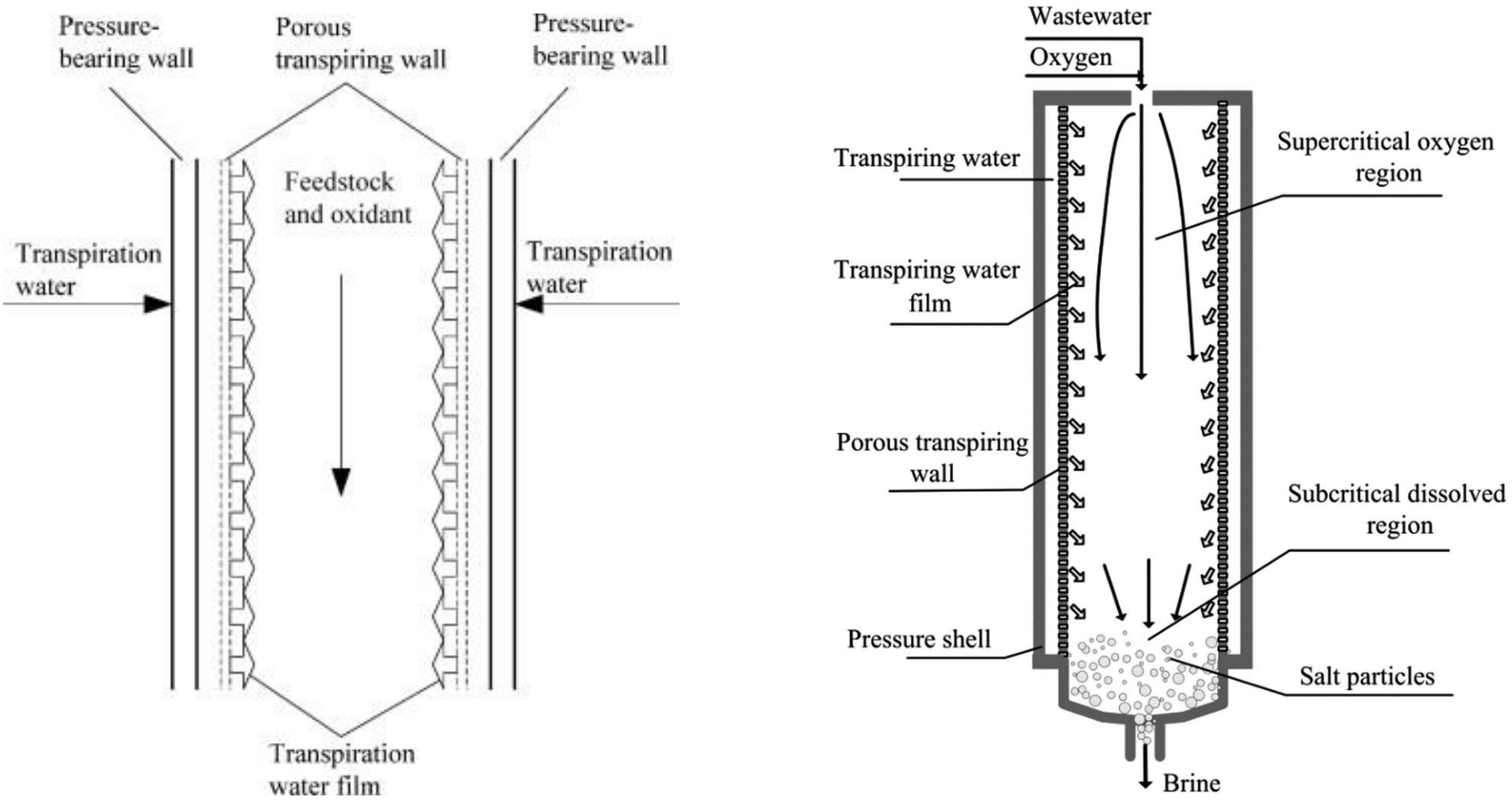

Figure 6: (a) Basic structure of TWR, adapted with permission from [90]; (b) Solid precipitation in TWR, adapted with permission from [91]

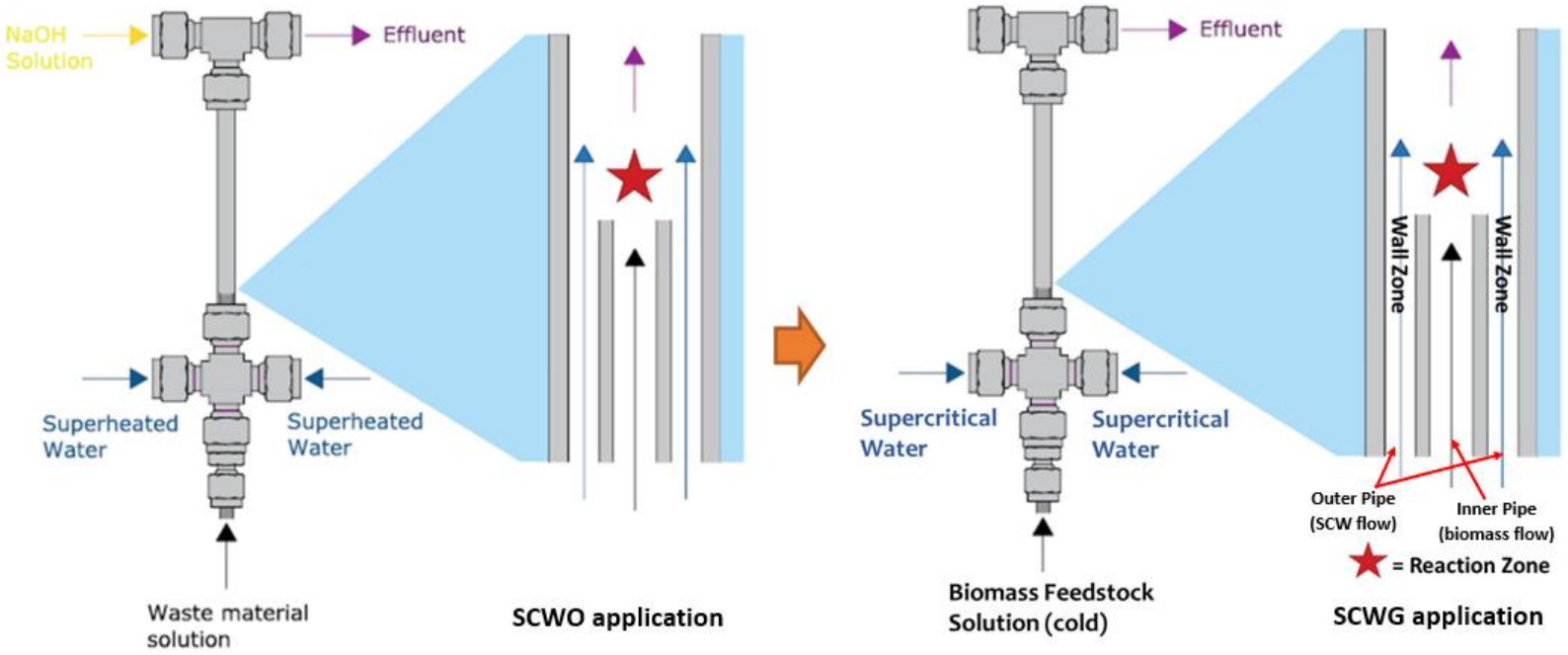

Figure 7: Schematic of the co-current mixing reactors used for the SCWO (left) and proposed for the SCWG (right), adapted with permission from [73]

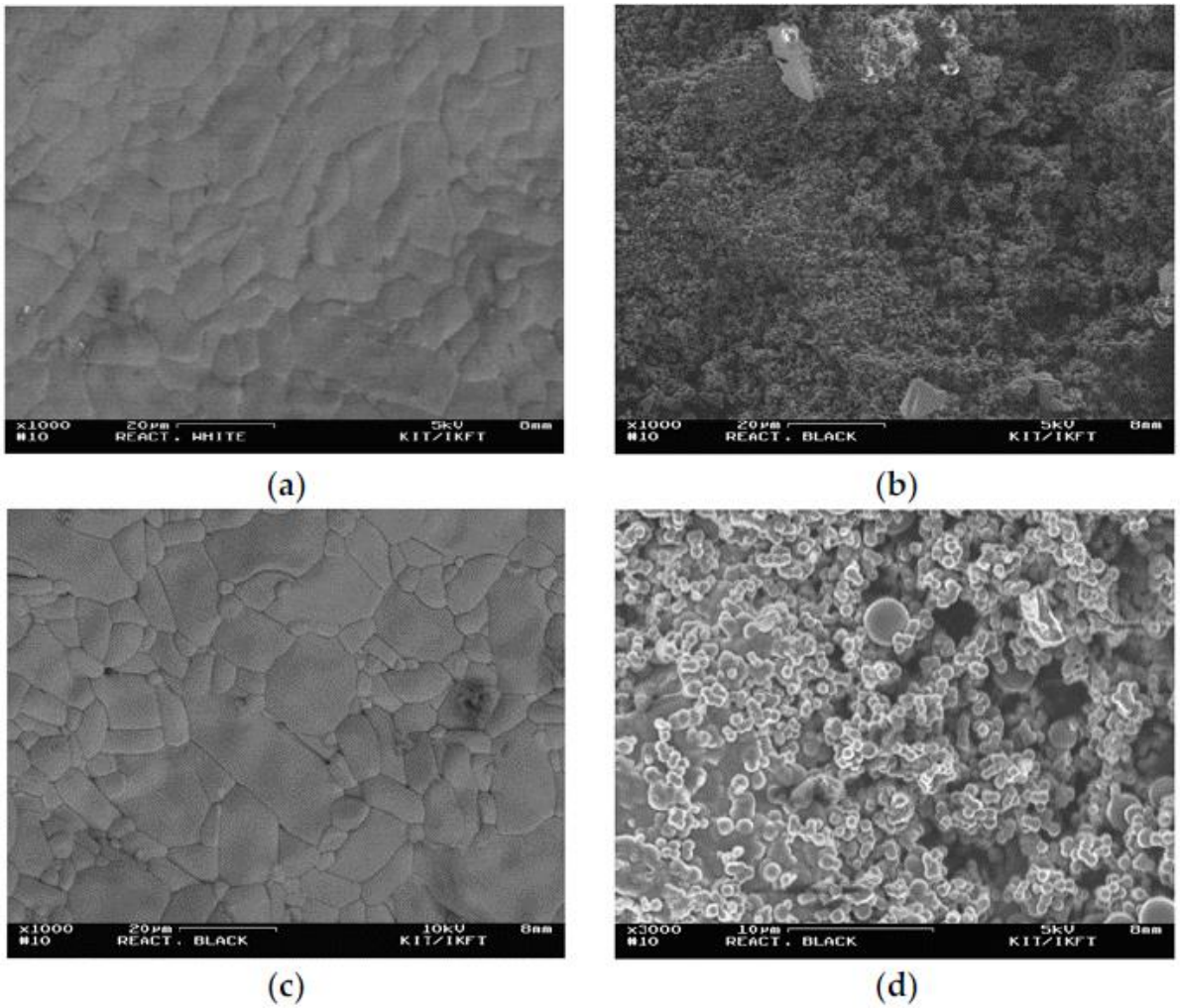

Figure 8: SEM images of the inner part of the ceramic inlay before and after the experiment: (**a**) surface before the experiment (1000×); (**b**) surface after the experiment, black area (1000×); (**c**) surface after the experiment and after washed with acetone, white area (1000×); and (**d**) surface after the experiment, black area (3000×), adapted with permission from [88]

References:

[1] S.N. Reddy, S. Nanda, A.K. Dalai, J.A. Kozinski, Supercritical water gasification of biomass for hydrogen production, Int. J. Hydrogen Energy. 39 (2014) 6912–6926. https://doi.org/https://doi.org/10.1016/j.ijhydene.2014.02.125.

[2] T.G. Madenoglu, S. Kurt, M. Saglam, M. Yüksel, D. Gökkaya, L. Ballice, Hydrogen production from some agricultural residues by catalytic subcritical and supercritical water gasification, J. Supercrit. Fluids. (2012). https://doi.org/10.1016/j.supflu.2012.02.031.

[3] O. Yakaboylu, J. Harinck, K. Smit, W. de Jong, Supercritical Water Gasification of Biomass: A Literature and Technology Overview, Energies. 8 (2015) 859–894. https://doi.org/10.3390/en8020859.

[4] D. Yamaguchi, P.J. Sanderson, S. Lim, L. Aye, Supercritical water gasification of Victorian brown coal: Experimental characterisation, Int. J. Hydrogen Energy. (2009). https://doi.org/10.1016/j.ijhydene.2009.02.026.

[5] B.R. Pinkard, D. J. Gorman, K. Tiwari, J. C. Kramlich, P. G. Reinhall, I. V. Novosselov, Review of Gasification of Organic Compounds in Continuous-Flow, Supercritical Water Reactors, Ind. & Eng. Chem. Res. 57 (2018) 3471–3481. https://doi.org/10.1021/acs.iecr.8b00068.

[6] S.N. Reddy, S. Nanda, A.K. Dalai, J.A. Kozinski, Supercritical water gasification of biomass for hydrogen production, Int. J. Hydrogen Energy. (2014). https://doi.org/10.1016/j.ijhydene.2014.02.125.

[7] P. Azadi, R. Farnood, Review of heterogeneous catalysts for sub- and supercritical water gasification of biomass and wastes, Int. J. Hydrogen Energy. (2011). https://doi.org/10.1016/j.ijhydene.2011.05.081.

[8] C. Rodriguez Correa, A. Kruse, Supercritical water gasification of biomass for hydrogen production – Review, J. Supercrit. Fluids. 133 (2018) 573–590. https://doi.org/https://doi.org/10.1016/j.supflu.2017.09.019.

[9] J.A. Okolie, R. Rana, S. Nanda, A.K. Dalai, J.A. Kozinski, Supercritical water gasification of biomass: a state-of-the-art review of process parameters, reaction mechanisms and catalysis, Sustain. Energy Fuels. 3 (2019) 578–598. https://doi.org/10.1039/C8SE00565F.

[10] B.R. Pinkard, D.J. Gorman, K. Tiwari, E.G. Rasmussen, J.C. Kramlich, P.G. Reinhall, I. V Novosselov, Supercritical water gasification: practical design strategies and operational challenges for lab-scale, continuous flow reactors, Heliyon. 5 (2019) e01269–e01269. https://doi.org/10.1016/j.heliyon.2019.e01269.

[11] A. Demirbas, Hydrogen-rich gas from fruit shells via supercritical water extraction, Int. J. Hydrogen Energy. (2004). https://doi.org/10.1016/j.ijhydene.2003.11.012.

[12] S. Nanda, J. Isen, A.K. Dalai, J.A. Kozinski, Gasification of fruit wastes and agro-food residues in supercritical water, Energy Convers. Manag. 110 (2016) 296–306. https://doi.org/10.1016/j.enconman.2015.11.060.

[13] S. Nanda, R. Rana, H.N. Hunter, Z. Fang, A.K. Dalai, J.A. Kozinski, Hydrothermal catalytic processing of waste cooking oil for hydrogen-rich syngas production, Chem. Eng. Sci. (2019) 935–945. https://doi.org/10.1016/j.ces.2018.10.039.

[14] H. Su, E. Kanchanatip, D. Wang, R. Zheng, Z. Huang, Y. Chen, I. Mubeen, M. Yan, Production of H2-rich syngas from gasification of unsorted food waste in supercritical water, Waste Manag. (2020). https://doi.org/10.1016/j.wasman.2019.11.018.

[15] D. Elif, A. Nezihe, Hydrogen production by supercritical water gasification of fruit pulp in the presence of Ru/C, Int. J. Hydrogen Energy. 41 (2016) 8073–8083. https://doi.org/10.1016/j.ijhydene.2015.12.005.

[16] F. Safari, N. Javani, Z. Yumurtaci, Hydrogen production via supercritical water gasification of almond shell over algal and agricultural hydrochars as catalysts, Int. J. Hydrogen Energy. (2018). https://doi.org/10.1016/j.ijhydene.2017.05.102.

[17] H. Su, E. Kanchanatip, D. Wang, H. Zhang, Antoni, I. Mubeen, Z. Huang, M. Yan, Catalytic gasification of food waste in supercritical water over La promoted Ni/Al2O3 catalysts for enhancing H2 production, Int. J. Hydrogen Energy. 45 (2020) 553–564. https://doi.org/https://doi.org/10.1016/j.ijhydene.2019.10.219.

[18] S. Nanda, M. Gong, H.N. Hunter, A.K. Dalai, I. Gökalp, J.A. Kozinski, An assessment of pinecone gasification in subcritical, near-critical and supercritical water, Fuel Process. Technol. 168 (2017) 84–96. https://doi.org/10.1016/j.fuproc.2017.08.017.

[19] S. Nanda, S.N. Reddy, A.K. Dalai, J.A. Kozinski, Subcritical and supercritical water gasification of lignocellulosic biomass impregnated with nickel nanocatalyst for hydrogen production, Int. J. Hydrogen Energy. (2016). https://doi.org/10.1016/j.ijhydene.2015.10.060.

[20] A. Kumar, S. N. Reddy, In Situ Sub- and Supercritical Water Gasification of Nano-Nickel (Ni2+) Impregnated Biomass for H2 Production, Ind. & Eng. Chem. Res. 58 (2019) 4780–4793. https://doi.org/10.1021/acs.iecr.9b00425.

[21] S. Nanda, S.N. Reddy, D.V.N. Vo, B.N. Sahoo, J.A. Kozinski, Catalytic gasification of wheat straw in hot compressed (subcritical and supercritical) water for hydrogen production, Energy Sci. Eng. 6 (2018) 448–459. https://doi.org/10.1002/ese3.219.

[22] A. Kumar, S.N. Reddy, Subcritical and supercritical water in-situ gasification of metal (Ni/Ru/Fe) impregnated banana pseudo-stem for hydrogen rich fuel gas mixture, Int. J. Hydrogen Energy. 45 (2020) 18348–18362. https://doi.org/https://doi.org/10.1016/j.ijhydene.2019.08.009.

[23] J.A. Okolie, S. Nanda, A.K. Dalai, J.A. Kozinski, Hydrothermal gasification of soybean straw and flax straw for hydrogen-rich syngas production: Experimental and thermodynamic modeling, Energy Convers. Manag. 208 (2020) 112545. https://doi.org/https://doi.org/10.1016/j.enconman.2020.112545.

[24] Y.J. Lu, L.J. Guo, C.M. Ji, X.M. Zhang, X.H. Hao, Q.H. Yan, Hydrogen production by biomass gasification in supercritical water: A parametric study,

Int. J. Hydrogen Energy. (2006). https://doi.org/10.1016/j.ijhydene.2005.08.011.

[25] Y.J. Lu, H. Jin, L.J. Guo, X.M. Zhang, C.Q. Cao, X. Guo, Hydrogen production by biomass gasification in supercritical water with a fluidized bed reactor, Int. J. Hydrogen Energy. (2008). https://doi.org/10.1016/j.ijhydene.2008.07.082.

[26] N. Ding, R. Azargohar, A.K. Dalai, J.A. Kozinski, Catalytic gasification of cellulose and pinewood to H2 in supercritical water, Fuel. (2014). https://doi.org/10.1016/j.fuel.2013.11.021.

[27] C. Chen, Y.-Q. Jin, J.-H. Yan, Y. Chi, Simulation of municipal solid waste gasification in two different types of fixed bed reactors, Fuel. 103 (2013) 58–63. https://doi.org/https://doi.org/10.1016/j.fuel.2011.06.075.

[28] N. Akiya, P. E. Savage, Roles of Water for Chemical Reactions in High-Temperature Water, Chem. Rev. 102 (2002) 2725–2750. https://doi.org/10.1021/cr000668w.

[29] Y. Guo, S.Z. Wang, D.H. Xu, Y.M. Gong, H.H. Ma, X.Y. Tang, Review of catalytic supercritical water gasification for hydrogen production from biomass, Renew. Sustain. Energy Rev. (2010). https://doi.org/10.1016/j.rser.2009.08.012.

[30] Y. Lu, L. Guo, X. Zhang, C. Ji, Hydrogen production by supercritical water gasification of biomass: Explore the way to maximum hydrogen yield and high carbon gasification efficiency, Int. J. Hydrogen Energy. (2012). https://doi.org/10.1016/j.ijhydene.2011.11.064.

[31] S. Sivasangar, Z. Zainal, A. Salmiaton, Y.H. Taufiq-Yap, Supercritical water gasification of empty fruit bunches from oil palm for hydrogen production, Fuel. 143 (2015) 563–569. https://doi.org/10.1016/j.fuel.2014.11.073.

[32] F. Safari, M. Salimi, A. Tavasoli, A. Ataei, Non-catalytic conversion of wheat straw, walnut shell and almond shell into hydrogen rich gas in supercritical water media, Chinese J. Chem. Eng. (2016). https://doi.org/10.1016/j.cjche.2016.03.002.

[33] M. Osada, A. Yamaguchi, N. Hiyoshi, O. Sato, M. Shirai, Gasification of Sugarcane Bagasse over Supported Ruthenium Catalysts in Supercritical Water, Energy & Fuels. 26 (2012) 3179–3186. https://doi.org/10.1021/ef300460c.

[34] R.F. Susanti, L.W. Dianningrum, T. Yum, Y. Kim, B.G. Lee, J. Kim, High-yield hydrogen production from glucose by supercritical water gasification without added catalyst, Int. J. Hydrogen Energy. 37 (2012) 11677–11690. https://doi.org/https://doi.org/10.1016/j.ijhydene.2012.05.087.

[35] G. Chen, J. Andries, Z. Luo, H. Spliethoff, Biomass pyrolysis/gasification for product gas production: the overall investigation of parametric effects, Energy Convers. Manag. 44 (2003) 1875–1884. https://doi.org/https://doi.org/10.1016/S0196-8904(02)00188-7.

[36] M. Rashidi, A. Tavasoli, Hydrogen rich gas production via supercritical water gasification of sugarcane bagasse using unpromoted and copper promoted Ni/CNT nanocatalysts, J. Supercrit. Fluids. (2015). https://doi.org/10.1016/j.supflu.2015.01.008.

[37] M. Salimi, F. Safari, A. Tavasoli, A. Shakeri, Hydrothermal gasification of different agricultural wastes in supercritical water media for hydrogen production: a comparative study, Int. J. Ind. Chem. 7 (2016) 277–285. https://doi.org/10.1007/s40090-016-0091-y.

[38] Y. Hu, M. Gong, X. Xing, H. Wang, Y. Zeng, C.C. Xu, Supercritical water gasification of biomass model compounds: A review, Renew. Sustain. Energy Rev. 118 (2020) 109529. https://doi.org/https://doi.org/10.1016/j.rser.2019.109529.

[39] T. Güngören Madenoɨlu, E. Yildirir, M. Saɨlam, M. Yüksel, L. Ballice, Improvement in hydrogen production from hard-shell nut residues by catalytic hydrothermal gasification, J. Supercrit. Fluids. (2014). https://doi.org/10.1016/j.supflu.2014.09.033.

[40] T. Güngören Madenoğlu, N. Boukis, M. Sağlam, M. Yüksel, Supercritical water gasification of real biomass feedstocks in continuous flow system, Int. J. Hydrogen Energy. (2011). https://doi.org/10.1016/j.ijhydene.2011.08.047.

[41] T. Yoshida, Y. Matsumura, Gasification of Cellulose, Xylan, and Lignin Mixtures in Supercritical Water, Ind. & Eng. Chem. Res. 40 (2001) 5469–

5474. https://doi.org/10.1021/ie0101590.

[42] T. Güngören Madenoğlu, M. Sağlam, M. Yüksel, L. Ballice, Hydrothermal gasification of biomass model compounds (cellulose and lignin alkali) and model mixtures, J. Supercrit. Fluids. 115 (2016) 79–85. https://doi.org/https://doi.org/10.1016/j.supflu.2016.04.017.

[43] D. Castello, A. Kruse, L. Fiori, Low temperature supercritical water gasification of biomass constituents: Glucose/phenol mixtures, Biomass and Bioenergy. 73 (2015) 84–94. https://doi.org/https://doi.org/10.1016/j.biombioe.2014.12.010.

[44] T. Yoshida, Y. Oshima, Y. Matsumura, Gasification of biomass model compounds and real biomass in supercritical water, Biomass and Bioenergy. 26 (2004) 71–78. https://doi.org/https://doi.org/10.1016/S0961-9534(03)00063-1.

[45] D. Castello, A. Kruse, L. Fiori, Supercritical Water Gasification of Glucose/Phenol Mixtures as Model Compounds for Ligno-Cellulosic Biomass, Chem. Eng. Trans. 37 (2014) 193-198 SE-Research Articles. https://doi.org/10.3303/CET1437033.

[46] A.K. Goodwin, G.L. Rorrer, Conversion of Xylose and Xylose−Phenol Mixtures to Hydrogen-Rich Gas by Supercritical Water in an Isothermal Microtube Flow Reactor, Energy & Fuels. 23 (2009) 3818–3825. https://doi.org/10.1021/ef900227u.

[47] J. Yanik, S. Ebale, A. Kruse, M. Saglam, M. Yüksel, Biomass gasification in supercritical water: II. Effect of catalyst, Int. J. Hydrogen Energy. (2008). https://doi.org/10.1016/j.ijhydene.2008.06.024.

[48] Y. Lu, H. Jin, R. Zhang, Evaluation of stability and catalytic activity of Ni catalysts for hydrogen production by biomass gasification in supercritical water, Carbon Resour. Convers. (2019). https://doi.org/10.1016/j.crcon.2019.03.001.

[49] J. Yanik, S. Ebale, A. Kruse, M. Saglam, M. Yüksel, Biomass gasification in supercritical water: Part 1. Effect of the nature of biomass, Fuel. (2007). https://doi.org/10.1016/j.fuel.2007.01.025.

[50] D. Castello, A. Kruse, L. Fiori, Biomass gasification in supercritical and subcritical water: The effect of the reactor material, Chem. Eng. J. (2013). https://doi.org/10.1016/j.cej.2013.04.119.

[51] H. Su, W. Liao, J. Wang, D. Hantoko, Z. Zhou, H. Feng, J. Jiang, M. Yan, Assessment of supercritical water gasification of food waste under the background of waste sorting: Influences of plastic waste contents, Int. J. Hydrogen Energy. 45 (2020) 21138–21147. https://doi.org/https://doi.org/10.1016/j.ijhydene.2020.05.256.

[52] K. Kang, R. Azargohar, A.K. Dalai, H. Wang, Hydrogen production from lignin, cellulose and waste biomass via supercritical water gasification: Catalyst activity and process optimization study, Energy Convers. Manag. 117 (2016) 528–537. https://doi.org/10.1016/j.enconman.2016.03.008.

[53] H. Jin, Y. Lu, L. Guo, X. Zhang, A. Pei, Hydrogen production by supercritical water gasification of biomass with homogeneous and heterogeneous catalyst, Adv. Condens. Matter Phys. 2014 (2014) 9.

[54] W. Su, C. Cai, P. Liu, W. Lin, B. Liang, H. Zhang, Z. Ma, H. Ma, Y. Xing, W. Liu, Supercritical water gasification of food waste: Effect of parameters on hydrogen production, Int. J. Hydrogen Energy. 45 (2020) 14744–14755. https://doi.org/https://doi.org/10.1016/j.ijhydene.2020.03.190.

[55] Y.H. Taufiq-Yap, S. Sivasangar, M. Surahim, Catalytic Supercritical Water Gasification of Empty Palm Fruit Bunches Using ZnO-Doped Ni–CaO Catalyst for Hydrogen Production, BioEnergy Res. 12 (2019) 1066–1076. https://doi.org/10.1007/s12155-019-10031-8.

[56] R. Mehrani, M. Barati, A. Tavasoli, A. Karimi, Hydrogen production via supercritical water gasification of bagasse using Ni–Cu/γ-Al2O3 nano-catalysts, Environ. Technol. 36 (2015) 1265–1272. https://doi.org/10.1080/09593330.2014.984771.

[57] P. Azadi, S. Khan, F. Strobel, F. Azadi, R. Farnood, Hydrogen production from cellulose, lignin, bark and model carbohydrates in supercritical water using nickel and ruthenium catalysts, Appl. Catal. B Environ. (2012). https://doi.org/10.1016/j.apcatb.2012.01.035.

[58] A.J. Byrd, S. Kumar, L. Kong, H. Ramsurn, R.B. Gupta, Hydrogen production from catalytic gasification of switchgrass biocrude in supercritical water, Int. J. Hydrogen Energy. (2011). https://doi.org/10.1016/j.ijhydene.2010.12.026.

[59] D.C. Elliott, Catalytic hydrothermal gasification of biomass, Biofuels, Bioprod. Biorefining. 2 (2008) 254–265. https://doi.org/https://doi.org/10.1002/bbb.74.

[60] B.R. Pinkard, D.J. Gorman, K. Tiwari, E.G. Rasmussen, J.C. Kramlich, P.G. Reinhall, I. V. Novosselov, Supercritical water gasification: practical design strategies and operational challenges for lab-scale, continuous flow reactors, Heliyon. (2019). https://doi.org/10.1016/j.heliyon.2019.e01269.

[61] S. Nanda, A.K. Dalai, F. Berruti, J.A. Kozinski, Biochar as an Exceptional Bioresource for Energy, Agronomy, Carbon Sequestration, Activated Carbon and Specialty Materials, Waste and Biomass Valorization. 7 (2016) 201–235. https://doi.org/10.1007/s12649-015-9459-z.

[62] I.-G. Lee, Effect of metal addition to Ni/activated charcoal catalyst on gasification of glucose in supercritical water, Int. J. Hydrogen Energy. 36 (2011) 8869–8877. https://doi.org/https://doi.org/10.1016/j.ijhydene.2011.05.008.

[63] I.-G. Lee, S.-K. Ihm, Catalytic Gasification of Glucose over Ni/Activated Charcoal in Supercritical Water, Ind. Eng. Chem. Res. 48 (2009) 1435–1442. https://doi.org/10.1021/ie8012456.

[64] K. Kang, R. Azargohar, A.K. Dalai, H. Wang, Systematic screening and modification of Ni based catalysts for hydrogen generation from supercritical water gasification of lignin, Chem. Eng. J. (2016). https://doi.org/10.1016/j.cej.2015.08.032.

[65] M. Osada, O. Sato, K. Arai, M. Shirai, Stability of Supported Ruthenium Catalysts for Lignin Gasification in Supercritical Water, Energy & Fuels. 20 (2006) 2337–2343. https://doi.org/10.1021/ef060356h.

[66] J.A. Onwudili, P.T. Williams, Hydrogen and methane selectivity during alkaline supercritical water gasification of biomass with ruthenium-alumina

catalyst, Appl. Catal. B Environ. (2013). https://doi.org/10.1016/j.apcatb.2012.11.033.

[67] J. Chen, W. Xu, F. Zhang, H. Zuo, J. E, K. Wei, G. Liao, Y. Fan, Thermodynamic and environmental analysis of integrated supercritical water gasification of coal for power and hydrogen production, Energy Convers. Manag. 198 (2019) 111927. https://doi.org/https://doi.org/10.1016/j.enconman.2019.111927.

[68] P.M. Ruya, R. Purwadi, S.S. Lim, Supercritical water gasification of sewage sludge for power generation– thermodynamic study on auto-thermal operation using Aspen Plus, Energy Convers. Manag. 206 (2020) 112458. https://doi.org/https://doi.org/10.1016/j.enconman.2019.112458.

[69] J. Louw, C.E. Schwarz, J.H. Knoetze, A.J. Burger, Thermodynamic modelling of supercritical water gasification: Investigating the effect of biomass composition to aid in the selection of appropriate feedstock material, Bioresour. Technol. 174 (2014) 11–23. https://doi.org/https://doi.org/10.1016/j.biortech.2014.09.129.

[70] R.R. Bommareddy, Y. Wang, N. Pearcy, M. Hayes, E. Lester, N.P. Minton, A. V Conradie, A Sustainable Chemicals Manufacturing Paradigm Using CO2 and Renewable H2, IScience. 23 (2020) 101218. https://doi.org/https://doi.org/10.1016/j.isci.2020.101218.

[71] P.W. Dunne, A.S. Munn, C.L. Starkey, T.A. Huddle, E.H. Lester, Continuous-flow hydrothermal synthesis for the production of inorganic nanomaterials, Philos. Trans. R. Soc. A Math. Phys. Eng. Sci. 373 (2015) 20150015. https://doi.org/10.1098/rsta.2015.0015.

[72] A. Al-Atta, T. Huddle, Y.G. Rodríguez, F. Mato, J. García-Serna, M.J. Cocero, R. Gomes, E. Lester, A techno-economic assessment of the potential for combining supercritical water oxidation with ‘in-situ’ hydrothermal synthesis of nanocatalysts using a counter current mixing reactor, Chem. Eng. J. 344 (2018) 431–440. https://doi.org/https://doi.org/10.1016/j.cej.2018.03.058.

[73] A. Al-Atta, J. Sierra-Pallares, T. Huddle, E. Lester, A potential co-current mixing reactor design for supercritical water oxidation, J. Supercrit. Fluids.

158 (2020) 104708. https://doi.org/https://doi.org/10.1016/j.supflu.2019.104708.

[74] A. Sınağ, A. Kruse, J. Rathert, Influence of the Heating Rate and the Type of Catalyst on the Formation of Key Intermediates and on the Generation of Gases During Hydropyrolysis of Glucose in Supercritical Water in a Batch Reactor, Ind. & Eng. Chem. Res. 43 (2003) 502–508. https://doi.org/10.1021/ie030475+.

[75] E. Lester, G. Aksomaityte, J. Li, S. Gomez, J. Gonzalez-Gonzalez, M. Poliakoff, Controlled continuous hydrothermal synthesis of cobalt oxide (Co3O4) nanoparticles, Prog. Cryst. Growth Charact. Mater. 58 (2012) 3–13. https://doi.org/https://doi.org/10.1016/j.pcrysgrow.2011.10.008.

[76] A. Kruse, T. Henningsen, A. Sınağ, J. Pfeiffer, Biomass Gasification in Supercritical Water: Influence of the Dry Matter Content and the Formation of Phenols, Ind. & Eng. Chem. Res. 42 (2003) 3711–3717. https://doi.org/10.1021/ie0209430.

[77] P.A. Marrone, G.T. Hong, Corrosion control methods in supercritical water oxidation and gasification processes, J. Supercrit. Fluids. (2009). https://doi.org/10.1016/j.supflu.2009.08.001.

[78] S. Wang, D. Xu, Y. Guo, X. Tang, Y. Wang, J. Zhang, H. Ma, L. Qian, Y. Li, Supercritical Water Processing Technologies for Environment, Energy and Nanomaterial Applications, 1st ed., Springer Singapore, Singapore, 2020.

[79] A. Chuntanapum, Y. Matsumura, Formation of Tarry Material from 5-HMF in Subcritical and Supercritical Water, Ind. & Eng. Chem. Res. 48 (2009) 9837–9846. https://doi.org/10.1021/ie900423g.

[80] A. Kruse, Supercritical water gasification, Biofuels, Bioprod. Biorefining. 2 (2008) 415–437. https://doi.org/10.1002/bbb.93.

[81] Y. Matsumura, T. Minowa, B. Potic, S.R.A. Kersten, W. Prins, W.P.M. Van Swaaij, B. Van De Beld, D.C. Elliott, G.G. Neuenschwander, A. Kruse, M.J. Antal, Biomass gasification in near- and super-critical water: Status and prospects, Biomass and Bioenergy. (2005).

https://doi.org/10.1016/j.biombioe.2005.04.006.

[82] D. Selvi Gökkaya, M. Sert, M. Sağlam, M. Yüksel, L. Ballice, Hydrothermal gasification of the isolated hemicellulose and sawdust of the white poplar (Populus alba L.), J. Supercrit. Fluids. 162 (2020) 104846. https://doi.org/https://doi.org/10.1016/j.supflu.2020.104846.

[83] N. Boukis, U. Galla, H. Müller, E. Dinjus, Biomass gasification in supercritical water. Experimental progress achieved with the VERENA pilot plant, 15th Eur. Conf. Exhib. (2008).

[84] O. Yakaboylu, I. Albrecht, J. Harinck, K.G. Smit, G.A. Tsalidis, M. Di Marcello, K. Anastasakis, W. de Jong, Supercritical water gasification of biomass in fluidized bed: First results and experiences obtained from TU Delft/Gensos semi-pilot scale setup, Biomass and Bioenergy. 111 (2018) 330–342. https://doi.org/10.1016/j.biombioe.2016.12.007.

[85] P. D'Jesús, N. Boukis, B. Kraushaar-Czarnetzki, E. Dinjus, Gasification of corn and clover grass in supercritical water, Fuel. (2006). https://doi.org/10.1016/j.fuel.2005.10.022.

[86] P.A. Marrone, G.T. Hong, Corrosion control methods in supercritical water oxidation and gasification processes, J. Supercrit. Fluids. 51 (2009) 83–103. https://doi.org/https://doi.org/10.1016/j.supflu.2009.08.001.

[87] P. D'Jesús, N. Boukis, B. Kraushaar-Czarnetzki, E. Dinjus, Influence of Process Variables on Gasification of Corn Silage in Supercritical Water, Ind. & Eng. Chem. Res. 45 (2006) 1622–1630. https://doi.org/10.1021/ie050367i.

[88] D. Castello, B. Rolli, A. Kruse, L. Fiori, Supercritical Water Gasification of Biomass in a Ceramic Reactor: Long-Time Batch Experiments, Energies. 10 (2017) 1734. https://doi.org/10.3390/en10111734.

[89] AHDB, Hay and straw prices, Br. Hay Straw Merch. Assoc. (2020). https://ahdb.org.uk/dairy/hay-and-straw-prices.

[90] D. Xu, S. Wang, C. Huang, X. Tang, Y. Guo, Transpiring wall reactor in supercritical water oxidation, Chem. Eng. Res. Des. 92 (2014) 2626–2639. https://doi.org/https://doi.org/10.1016/j.cherd.2014.02.028.

[91] S. Wang, D. Xu, Y. Guo, X. Tang, Y. Wang, J. Zhang, H. Ma, L. Qian, Y. Li, Study on Salt Deposition and Crystallization Properties in Sub/Supercritical Water, in: Supercrit. Water Process. Technol. Environ. Energy Nanomater. Appl., Springer Singapore, Singapore, 2020: pp. 261–303. https://doi.org/10.1007/978-981-13-9326-6_7.